ILC School Erice Linac I
Lecture Notes

Peter Tenenbaum
DRAFT August 30, 2007

Contents

1 The Electromagnetic Wave Equation in Vacuum

The acceleration of the electron and positron beams in the International Linear Collider (ILC) is accomplished by radio-frequency (RF) electromagnetic fields which are stored in multi-cell accelerating cavities (aka "accelerator structures," or, more archaically, "disc-loaded wave guides"). To see why this is the case, it is necessary to begin with Maxwell's equations. Note that these class notes will always use *Système International* (SI) units – meters, kilograms, seconds, and amperes. Other lecturers and/or classes may use various other systems, such as Gaussian units, for electromagnetism, but in the linac classes voltages are real volts and currents are real amperes.

1.1 Maxwell's Equations in SI

Any discussion of the applications of time-dependent electromagnetic fields must begin with Maxwell's equations [1]:

$$\begin{aligned}
\vec{\nabla} \cdot \vec{D} &= \rho, \\
\vec{\nabla} \cdot \vec{B} &= 0, \\
\vec{\nabla} \times \vec{H} &= \vec{J} + \frac{\partial \vec{D}}{\partial t}, \\
\vec{\nabla} \times \vec{E} &= -\frac{\partial \vec{B}}{\partial t}.
\end{aligned} \tag{1}$$

In Equation 1, the four electromagnetic vectors $\vec{E}$, $\vec{D}$, $\vec{B}$, $\vec{H}$ are all present, and MKSA units are assumed. The number of vector quantities can be reduced by replacing $\vec{B}$ with $\mu\vec{H}$ and replacing $\vec{D}$ with $\epsilon\vec{E}$.

1.2 The Wave Equation

Maxwell's equation can be combined into a wave equation by making use of the vector identity:

$$\vec{\nabla} \times (\vec{\nabla} \times \vec{A}) \equiv \vec{\nabla}(\vec{\nabla} \cdot \vec{A}) - \nabla^2 \vec{A}. \tag{2}$$

Let us apply the identity above to the Maxwell's electric field curl equation:

$$\begin{aligned} \vec{\nabla} \times (\vec{\nabla} \times \vec{E}) &= \vec{\nabla}(\vec{\nabla} \cdot \vec{E}) - \nabla^2 \vec{E} \\ &= -\vec{\nabla} \times \frac{\partial \vec{B}}{\partial t}. \end{aligned} \tag{3}$$

In a region of space free of charges, $\vec{\nabla} \cdot \vec{E} = 0$. Assuming that we are only interested in well-behaved analytic functions (ie, those for which we can reverse the order of differentiations with impunity), we can transform the magnetic field term in Equation 3 from the curl of a time derivative to the time derivative of a curl:

$$\nabla^2 \vec{E} = \frac{\partial}{\partial t} \vec{\nabla} \times \vec{B}. \tag{4}$$

If we replace $\vec{B}$ with $\mu\vec{H}$, then the RHS of Equation 4 can be replaced with the Maxwell's magnetic curl equation:

$$\begin{aligned} \nabla^2 \vec{E} &= \mu \frac{\partial}{\partial t} \vec{\nabla} \times \vec{H} \\ &= \mu \left[\frac{\partial^2 \vec{D}}{\partial t^2} + \frac{\partial \vec{J}}{\partial t} \right]. \end{aligned} \tag{5}$$

If we assume that the region of interest is also current-free, we can replace $\vec{D}$ with $\epsilon\vec{E}$ to obtain:

$$\nabla^2 \vec{E} - \mu\epsilon \frac{\partial^2 \vec{E}}{\partial t^2} = 0. \tag{6}$$

Equation 6 is a *wave equation* for the electric field. A similar process can be followed to obtain a wave equation for the magnetic field:

$$\nabla^2 \vec{H} - \mu\epsilon \frac{\partial^2 \vec{H}}{\partial t^2} = 0. \tag{7}$$

1.3 Solution to the Wave Equation in Free Space

Equations 6 and 7 can (almost!) be solved by inspection: the solutions will be superpositions of travelling plane waves. Let us define the z axis to be parallel to the direction of propagation. The form of the solution will then be:

$$\begin{aligned} \vec{E} &= \vec{E}_0 \exp[i(\omega t - kz)], \\ \vec{H} &= \vec{H}_0 \exp[i(\omega t - kz)]. \end{aligned} \tag{8}$$

If we consider solutions in free space (ie, no boundaries or boundary conditions), then since space is isotropic and homogeneous $\vec{E}_0$ and $\vec{H}_0$ must be constant over all time and all space.

Applying Equation 6 to the suggested solution in Equation 8, we find:

$$\nabla^2 \vec{E} = \left(\frac{\partial^2}{\partial x^2} + \frac{\partial^2}{\partial y^2} + \frac{\partial^2}{\partial z^2} \right) \vec{E}_0 \exp[i(\omega t - kz)] \tag{9}$$

$$= \mu\epsilon \frac{\partial^2}{\partial t^2} \vec{E}_0 \exp[i(\omega t - kz)].$$

Because $\vec{E}_0$ is constant over all time and space, both the laplacian and the time derivative operate only upon the complex exponential. After appropriate cancellation of the constant and the exponential itself, what remains is:

$$-k^2 = -\mu\epsilon\omega^2. \tag{10}$$

Equation 10 relates the wave number, $k \equiv 2\pi/\lambda$, to the angular frequency, $\omega \equiv 2\pi\nu$, for any wave which can propagate in free space. In particular, Equation 10 shows that the phase velocity of any such wave, ω/k, will be $1/\sqrt{\mu\epsilon}$, and it can also be easily shown that the group velocity, $\partial\omega/\partial k$, will also be $1/\sqrt{\mu\epsilon}$. In vacuum, it is well known that $1/\sqrt{\mu_0\epsilon_0} = c$. So: the solution is a wave which propagates in the z direction at the speed of light.

A problem appears when Equation 8 is subject to the other constraints of Maxwell's equations. Consider for example the electric divergence equation, which requires that in the absence of electric charges the divergence of the electric field must vanish. Since the solution in Equation 8 varies only in z, the divergence equation reduces to:

$$\vec{\nabla} \cdot \vec{E} = \frac{\partial E_z}{\partial z} = -ikE_{0,z} \exp[i(\omega t - kz)] = 0. \tag{11}$$

Equation 11 implies that either $E_{0,z}$ vanishes, or else the momentum vector k vanishes. Setting $k \equiv 0$ corresponds to electrostatic acceleration, which for engineering reasons is unacceptable for final energies of more than a few MeV. Setting $E_{0,z} \equiv 0$ corresponds to a purely transverse electric wave, which will accelerate charged particles normal to the direction of wave propagation. To see why this is unacceptable for accelerating anything, consider a particle which is already ultra-relativistic and therefore moving at a speed close to c; this particle interacts with a wave which propagates in z and has its electric field oriented along x; the interaction begins at $t = x = z = 0$; and the particle's initial direction of travel is also assumed to be parallel to $\hat{x}$. At $t = 0$, the electric field is $E_{0,x}$, and in a time dt the particle's energy gain is given by the product of the electric field and the distance over which the field is applied, or $\Delta U = E_{0,x}cdt$; the particle is accelerated in the $+x$ direction. One half-period later, the sign of the electric field is reversed and the change in kinetic energy is $\Delta U = -E_{0,x}cdt$. Thus, we see that the particle is alternately accelerated and decelerated in the x direction, and no net energy increase is possible.

If a solution of the form shown above – a travelling-wave solution – is to be used for accelerating particles, it will be necessary to arrange for the electric field parallel to the direction of travel to be nonzero. Equation 11 shows that the problem with the free-space solution is that the field parallel to the direction of travel must be zero to satisfy the electric divergence equation. This constraint can be relaxed by permitting $\vec{E}_0$ and $\vec{H}_0$ to be functions of the transverse coordinates. Since $\vec{\nabla} \cdot \vec{E} = \frac{\partial E_z}{\partial z} + \frac{\partial E_{0,x}}{\partial x} + \frac{\partial E_{0,y}}{\partial y} = 0$, allowing a solution where $\partial E_{0,x}/\partial x$ and/or $\partial E_{0,y}/\partial y$ are non-zero allows $\frac{\partial E_z}{\partial z}$ to be non-zero as well, thus leading to a solution with a nonzero electric field parallel to the direction of wave propagation. Arranging for transverse variation in $\vec{E}_0$ and $\vec{H}_0$, in turn, requires that the transverse symmetry of free space be broken by some form of boundary conditions. As a trial, let us consider a conducting circular pipe of inner radius b oriented along the z axis, such that the center of the pipe corresponds to $x = y = 0$. Because the pipe exhibits cylindrical symmetry, we will use cylindrical coordinates (r, θ, z) to explore this solution. Such a pipe is usually referred to as a *waveguide*.

2 Solution to the Wave Equation in a Regular Cylindrical Waveguide

To reiterate: we seek a solution to Maxwell's equations which is of the form:

$$\vec{E} = \vec{E}_0 \exp[i(\omega t - kz)], \qquad (12)$$
$$\vec{H} = \vec{H}_0 \exp[i(\omega t - kz)],$$

where $\vec{E}_0$ and $\vec{H}_0$ are functions of transverse coordinates r and θ, but not of z or t. By limiting ourselves to solutions of this form, we can make a few alterations in the way that z and t partial derivatives are presented:

$$\frac{\partial}{\partial z} = -ik, \ \frac{\partial^2}{\partial z^2} = -k^2, \qquad (13)$$
$$\frac{\partial}{\partial t} = i\omega, \ \frac{\partial^2}{\partial t^2} = -\omega^2.$$

2.1 Boundary Conditions

Let us consider a perfectly conducting hollow cylindrical pipe, infinitely long with radius b, as shown in Figure 1. What are the boundary conditions for the electric and magnetic fields at $r = b$, where the vacuum and the conductor meet?
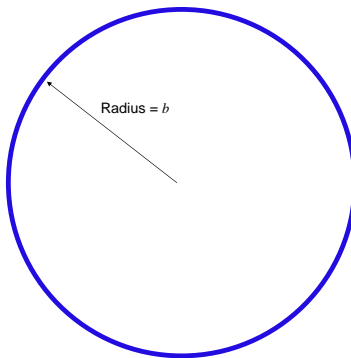
Figure 1: Infinitely-long pefectly-conducting cylinder of radius b, surrounding a vacuum.

The boundary conditions for electric and magnetic fields at *any* boundary between different media are that the *normal* component of $\vec{B}$ and the *tangential* component of $\vec{E}$ are continuous across the boundary [2]. The *normal* component of $\vec{E}$ across the boundary must obey the relations:

$$\epsilon_1 E_{1n} - \epsilon_2 E_{2n} = \Sigma, \qquad (14)$$
$$\sigma_1 E_{1n} - \sigma_2 E_{2n} = i\omega\Sigma,$$

where ϵ_1, ϵ_2 are the permeabilities of the two regions, σ_1, σ_2 are the conductivities of the two regions (with units of inverse ohms/meter in MKS units), and Σ is the surface charge density at the boundary. At the boundary between vacuum ($\sigma_1 \equiv 0$) and a perfect conductor ($\sigma_2 \equiv \infty$),

Equation 14 shows that the normal electric field in the conductor (here E_{2n}) must go to zero, while the normal electric field in the vacuum at the boundary must be equal to Σ/ϵ_0.

Within the body of the conductor, we can apply the magnetic curl equation: we can replace the current, $\vec{J}$, with $\sigma_2 \vec{E}_2$ (Ohm's Law) and the time derivative, $\partial \vec{E}_2/\partial t$, with $i\omega \vec{E}_2$, yielding:

$$\vec{E}_2 = \frac{1}{\sigma_2 + i\epsilon_2\omega} \vec{\nabla} \times \vec{H}_2. \tag{15}$$

Since $\sigma_2 \equiv \infty$ in a perfect conductor, and $\vec{H}_2$ is by definition finite, it therefore follows that $\vec{E}_2 \equiv 0$ everywhere in the conductor. Since the tangential component of $\vec{E}$ is continuous across the boundary, it follows that the tangential component of $\vec{E}$ is zero at the boundary. Since $\vec{E}_2 \equiv 0$, we can use Maxwell's electric curl equation to show that $\vec{B}_2$, and therefore $\vec{H}_2$, are identically zero throughout the conductor as well. From this we find that the normal component of $\vec{H}$ must go to zero at the boundary between vacuum and the conducting cylinder. Expressing this in cylindrical coordinates, then, we find that **at the boundary between vacuum and the perfect conductor ($r = b$), the field components E_θ, E_z, and H_r are required to go to zero** because the field inside the conductor is identically zero and the boundary conditions require these components to be continuous across the boundary.

Finally: since $E_\theta = 0$ at the boundary, Maxwell's magnetic curl equation shows that $(\vec{\nabla} \times \vec{H})_\theta = 0$. The θ component of $\vec{\nabla} \times \vec{H}$ is given by $\partial H_r/\partial z - \partial H_z/\partial r$. On the boundary, H_r is identically zero for all values of z, therefore $\partial H_r/\partial z = 0$ and in order for $(\vec{\nabla} \times \vec{H})_\theta$ to be zero, **it follows that $\partial H_z/\partial r = 0$ at the boundary.**

2.2 Solving for the Longitudinal Components

We can now solve Equation 6 for the case of the longitudinal components of $\vec{E}$ and $\vec{H}$. Let us begin with the electric field, and recall that we seek a solution of the form $E_z = E_{0,z}(r,\theta) \exp[i(\omega t - kz)]$. We can rewrite the z component of the wave equation thus:

$$\nabla_\perp^2 E_z - k^2 E_z + \mu\epsilon\omega^2 E_z = 0, \tag{16}$$

where we have defined the transverse component of the laplacian, $\nabla_\perp^2 \equiv \nabla^2 - \partial^2/\partial z^2$, and replaced the longitudinal and time derivatives as shown in Equation 13. We can further simplify Equation 16 by defining $k_c^2 \equiv \mu\epsilon\omega^2 - k^2$, and cancelling the common factor of $\exp[i(\omega t - kz)]$ from all terms:

$$\nabla_\perp^2 E_{0,z} + k_c^2 E_{0,z} = 0. \tag{17}$$

The solution to Equation 17 is straightforward, but tedious; interested students are directed to Appendix B. The result is a Fourier series containing sinusoids and Bessel functions:

$$E_{0,z} = \sum_{n=0}^{\infty} a_n J_n(k_c r) \cos(n\theta + \theta_n). \tag{18}$$

A similar solution can be derived for $H_{0,z}$.

2.3 Applying the Boundary Conditions

With a general solution for $E_{0,z}$ and $H_{0,z}$ in hand, we can now apply the necessary boundary conditions. The electric field boundary condition requires that $E_{0,z}$ vanish at $r = b$. This in turn

implies that $k_c b = z_{np}$, where z_{np} is the pth zero of J_n. The solution for $E_{0,z}$ is therefore more readily expressed as a double sum:

$$E_{0,z} = \sum_{p=1}^{\infty} \sum_{n=0}^{\infty} a_{np} J_n(k_{c,np} r) \cos(n\theta + \theta_{np}). \tag{19}$$

The constraint on k_c values has an interesting implication on the waves which flow in the waveguide. We can use this constraint in an expansion of k_c:

$$k_{c,np} = \frac{z_{np}}{b} = \sqrt{\mu\epsilon\omega^2 - k^2}. \tag{20}$$

Now consider the case in which $k^2 = 0$, corresponding to infinite wavelength. Equation 20 implies that the wave with infinite wavelength must have a nonzero frequency. We define this frequency to be the *cutoff frequency* of the waveguide:

$$\omega_c = \frac{1}{\sqrt{\mu\epsilon}} \frac{z_{np}}{b}. \tag{21}$$

This allows us to solve Equation 20 for k in terms of ω and ω_c:

$$k^2 = \mu\epsilon \left(\omega^2 - \omega_c^2 \right). \tag{22}$$

If a wave with a frequency greater than ω_c is introduced into our waveguide, Equation 22 tells us that k will be real-valued, as we require. If, on the other hand, $\omega < \omega_c$, then k will be imaginary. Substituting an imaginary value of k into Equation 12, we find that the solution no longer has the form of an oscillation in z, but rather an exponential decay or growth in z. If we sensibly reject the exponential-growth solution, the implication is that a wave with a frequency below the cutoff frequency decays exponentially in a waveguide. Such a wave is called an *evanescent* wave.

In summary, breaking the transverse symmetry of an electromagnetic plane wave via a waveguide permits a solution in which the longitudinal electric and magnetic fields do not vanish, but at the expense of forbidding waves with excessively low frequencies from propagating in the guide.

Additional complications can be observed if Equation 22 is used to compute the phase and group velocity of a wave in a waveguide. The group velocity, $d\omega/dk$, is given by:

$$v_{\mathrm{gr}} = \frac{d\omega}{dk} = \frac{1}{\sqrt{\mu\epsilon}} \frac{\sqrt{\omega^2 - \omega_c^2}}{\omega}. \tag{23}$$

Since $\sqrt{\omega^2 - \omega_c^2} < \omega$ for frequencies above cutoff, the group velocity is less than the speed of light, and is a function of frequency; asymptotically, as $\omega \to \infty$, the group velocity approaches the speed of light. The phase velocity, ω/k, is given by:

$$v_{\mathrm{ph}} = \frac{\omega}{k} = \sqrt{\frac{1}{\mu\epsilon} + \frac{\omega_c^2}{k^2}}. \tag{24}$$

The phase velocity, like the group velocity, is a function of frequency. Unlike the group velocity, the phase velocity is greater than the speed of light; indeed, it can be shown that the product of the phase velocity and the group velocity for any such wave is c^2. This means that the electromagnetic wave in a regular waveguide is unacceptable for use in accelerating particles despite its longitudinal electric field. This is because the particles in question will have velocities below that of light. As the wave and the particle travel down the waveguide, the accelerating phase of the wave will overtake

the particle and the decelerating phase will catch up with the particle; as with the transverse wave described previously, over one oscillation this wave will provide equal acceleration and deceleration, for a net acceleration of zero.

By analogy with the longitudinal electric field solution, we can derive a solution to the longitudinal magnetic field, $H_{0,z}$:

$$H_{0,z} = \sum_{v=1}^{\infty} \sum_{u=0}^{\infty} f_{uv} J_u(k_{c,uv} r) \cos(u\theta + \theta_{uv}). \tag{25}$$

Because its boundary conditions are different, the cutoff wave number $k_{c,uv}$ is different from the electric field cutoff. In particular, since it is the radial derivative of the field which vanishes at the boundary, we find for the magnetic field that $k_{c,uv} b = y_{uv}$, where y_{uv} is the vth zero of J_u', and $J_u'(\mathcal{R}) \equiv dJ_u(\mathcal{R})/d\mathcal{R}$.

2.4   TE and TM Modes

Although electromagnetic waves in a regular waveguide are not suitable for acceleration, they have many other useful characteristics (for example, waveguides can be used to transport waves from a source to a more suitable accelerating structure). Furthermore, we will find that the waves which are ultimately suitable for acceleration share many characteristics with those described above. For this reason, we will complete our study of electromagnetic waves in regular circular waveguide.

As we saw in the previous section, the longitudinal electric and magnetic field components will have different dispersion relations and cutoff wave numbers due to the fact that the cutoff wave numbers for the electric field are proportional to the zeroes of the Bessel functions J_n, while the cutoff wave numbers for the magnetic field are proportional to the zeroes of the Bessel function derivatives J_n' (note: "dispersion relation" is a fancy term which means "relation between ω and k"). This in turn means that, given a wave with frequency ω propagating in a cylindrical waveguide, *the eigenmodes of the waveguide cannot have both a longitudinal electric field and a longitudinal magnetic field.* A mode which has a longitudinal electric field (and thus no longitudinal magnetic field) is called a "Transverse Magnetic" mode, or TM mode; a mode which has a longitudinal electric field is called a "Transverse Electric" or TE mode.

TE and TM modes are usually specified by the TE or TM name and two integers in subscripts, thus TM_{np} or TE_{uv}. The subscripts, n, p, u, v are defined in Equations 19 and 25. Physically, the first integer (n or u) tells the number of nulls in the field pattern around the azimuth (to be precise, the number of nulls is $2n$ or $2u$), while the second integer (p or v) tells the number of nulls encountered radially between $r = 0$ and $r = b$.

2.5   Fields of the TM_{np} Mode

As shown in Equation 19, the longitudinal electric field of a TM_{np} mode is given by:

$$E_{0,z} = J_n(k_{c,np} r) \cos(n\theta + \theta_{np}), \tag{26}$$

while the longitudinal magnetic field component, $H_{0,z}$, is known to be identically zero. It is now possible to solve for all 6 components of the TM_{np} mode. The solution is presented here; those interested in the mathematics of solving for the remaining components are directed to Appendix C.

$$
\begin{aligned}
E_{0,z} &= J_n(k_{c,np} r) \cos(n\theta + \theta_{np}), \\
H_{0,z} &= 0,
\end{aligned}
\tag{27}
$$

$$E_{0,r} = \frac{-ik}{k_{c,np}} J_n'(k_{c,np}r)\cos(n\theta + \theta_{np}),$$

$$E_{0,\theta} = \frac{ikn}{k_{c,np}^2 r} J_n(k_{c,np}r)\sin(n\theta + \theta_{np}),$$

$$H_{0,r} = \frac{-i\omega\epsilon n}{k_{c,np}^2 r} J_n(k_{c,np}r)\sin(n\theta + \theta_{np}),$$

$$H_{0,\theta} = \frac{-i\omega\epsilon}{k_{c,np}} J_n'(k_{c,np}r)\cos(n\theta + \theta_{np}).$$

A similar painful procedure can be used to derive the fields of a TE mode. We point out that for $n \neq 0$ there are two polarizations possible for each TE or TM mode; the second polarization can be obtained from Equation 27 by replacing sine with cosine and cosine with -sine.

Table 3 Mode Patterns in Circular Waveguide.

Wave Type	TM$_{01}$	TM$_{02}$	TM$_{11}$	TE$_{01}$	TE$_{11}$
Field distributions in cross-sectional plane, at plane of maximum transverse fields			Distributions below along this plane		Distributions below along this plane
Field distributions along guide					
Field components present	E_z, E_r, H_ϕ	E_z, E_r, H_ϕ	E_z, E_r, E_ϕ, H_r, H_ϕ	H_z, H_r, E_ϕ	H_z, H_r, H_ϕ, E_r, E_ϕ

7–98
8355A213

Figure 2: Field patterns for several TE and TM modes in circular waveguide.

Figure 2 shows the field patterns associated with several of the lower TE and TM modes. Figure 3 shows the relationship between cutoff frequencies for various modes in a circular waveguide. Note that the TE$_{11}$ mode has the lowest cutoff; frequencies which are so low that they can only propagate in the TE$_{11}$ mode are called *single-moded* for this reason.

3   Single-Celled Accelerating Cavities

In section 1.3, we saw that in free space waves of any frequency can propagate; that both the phase velocity and the group velocity of such waves are the speed of light; and that such waves have a purely transverse polarization, so that they are not usable for acceleration of charged particles. In section 2 we saw that in a regular cylindrical waveguide only waves above the cutoff frequency can propagate; that such waves can have a longitudinal electric field component; that the group velocity of such waves are below the speed of light, but that the phase velocity is above the speed of light. Thus, a regular waveguide is also an unacceptable device for acceleration of beams.

The problem with the regular waveguide is that, with a phase velocity exceeding c, the accelerating phase of the wave will overtake the particles which are to be accelerated, and ultimately the decelerating phase will overlap those particles. One solution, then is to consider using the accelerating phase to accelerate the particles, and then to separate the wave from the particles before the
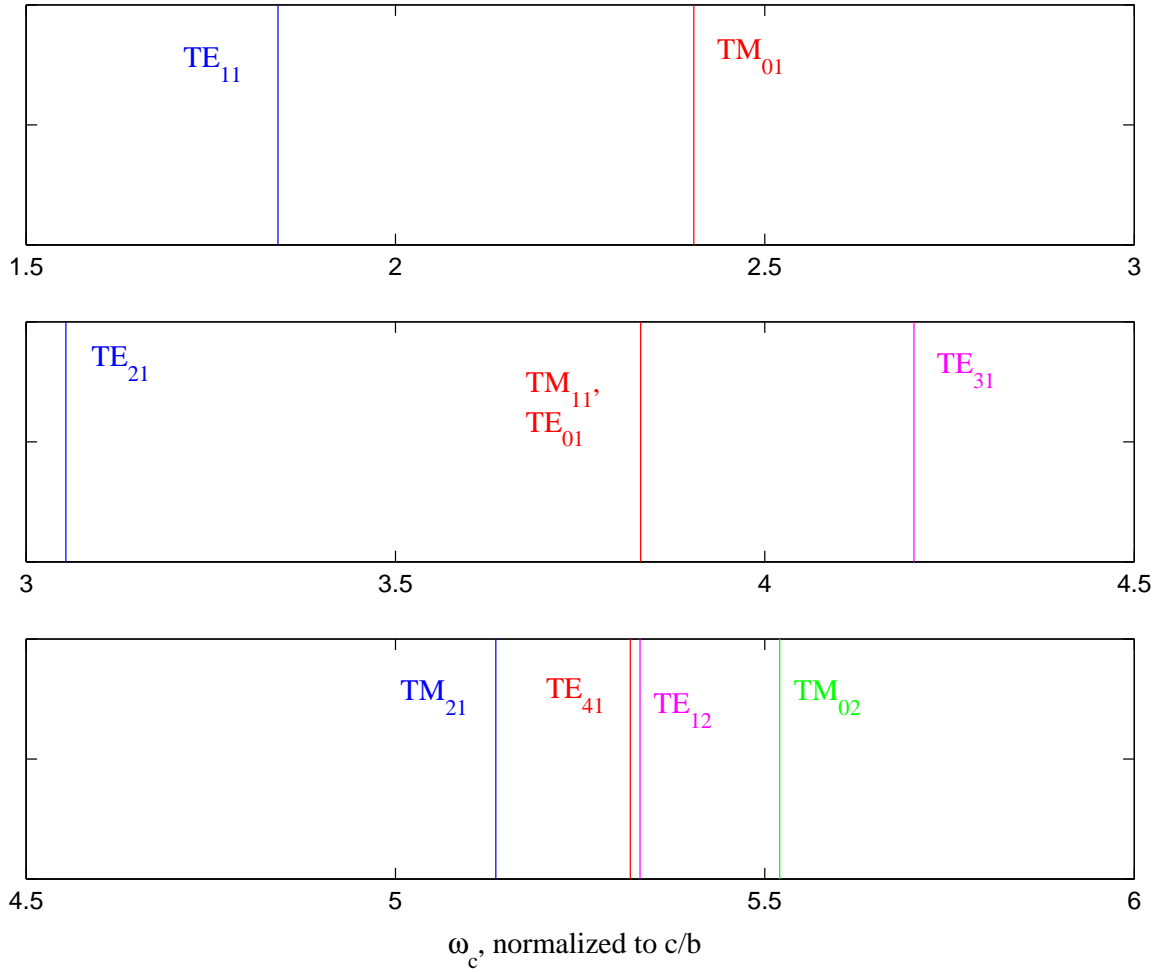
9

Figure 3: Cutoff frequencies ω_c normalized to c/b for the lowest 10 modes in circular waveguide.

decelerating phase can interact with them. This, in turn means applying a boundary condition to the only "free" axis present in the problem – the z axis.
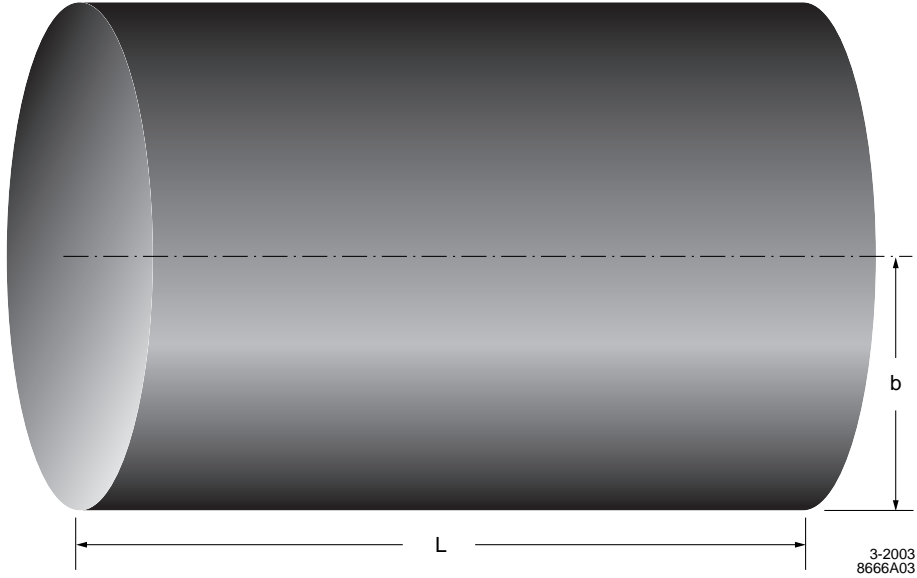

Figure 4: Perfectly-conducting right-circular cylinder with radius b and length L.

Consider a perfectly conducting right-circular cylinder of radius b and length L, as shown in Figure 4. It is immediately clear that any solution to Maxwell's equations must satisfy the boundary conditions for a regular circular waveguide of radius b. In addition, the conducting ends ("endcaps") of the cylinder imply additional boundary conditions:

- At $z = 0$ and $z = L$, the transverse electric field components, E_r and E_θ, must go to zero, since the electric field must be normal to any conducting boundary.

- At $z = 0$ and $z = L$, the longitudinal magnetic field component must go to zero, since the magnetic field must be tangential to any conducting boundary.

- Since the transverse components of $\vec{E}$ are identically zero on the endcaps, the transverse components of $\vec{\nabla} \times \vec{H}$ must also be zero there. We also know that H_z is identically zero at all of these locations. We therefore deduce that $\partial H_\theta / \partial z$ and $\partial H_r / \partial z$ must be zero at the endcaps.

What sort of solution will satisfy all of these requirements? Let us consider first a solution which is based on the TM_{01} mode: from inspection of Equation 27, we see that H_z, E_θ, and H_r are identically zero for this mode, so already we have satisfied the E_θ, H_z, and $\partial H_r / \partial z$ requirements on the endcaps, and of course the TM_{01} mode automatically satisfies the boundary conditions on the barrel.

Suppose that we now superimpose two TM_{01} waves within our cavity: one which is rightward-propagating, with $k \geq 0$, and another which is leftward-propagating, with a k value equal and opposite to the first. The resulting values of E_z, E_r, and H_θ become:

$$
\begin{aligned}
E_z &= J_0(k_{c,01} r) \cos(kz) \exp(i\omega t), & (28) \\
E_r &= \frac{-k}{k_{c,01}} J_0'(k_{c,01} r) \sin(kz) \exp(i\omega t),
\end{aligned}
$$

11

$$H_\theta = \frac{-i\omega\epsilon}{k_{c,01}} J_0'(k_{c,01}r)\cos(kz)\exp(i\omega t).$$

The first thing to notice about the fields in Equation 28 is that they no longer represent a traveling wave solution to Maxwell's equations: at $z = \pi/(2k)$, the longitudinal electric field E_z is identically zero for all time, while in a traveling wave solution the field at any z location would oscillate over time between zero and the maximum amplitude of the field. The second thing to notice is that, at $z = 0$, the fields in Equation 28 automatically satisfy the conducting boundary requirements: $E_r = \partial H_\theta/\partial z = 0$. The only remaining conditions are the conducting boundary conditions at $z = L$. These in turn can be satisfied if $kL = j\pi$, where j is an integer. The solution in Equation is known as a TM_{npj} mode: the first two indices are defined as they are for the traveling wave TM_{np} mode; the third index, j, tells the number of field nulls in the longitudinal dimension between $z = 0$ and $z = L$. Note that $j = 0$ is an allowed solution.

Another feature of the TM_{npj} mode is that, unlike the TM_{np} mode, only certain discrete frequencies can be sustained in the cavity. While the TM_{np} mode will support any frequency above $\omega_c \equiv z_{np}/b\sqrt{\mu\epsilon}$, the TM_{npj} mode will only support TM_{np} modes for which $kL = j\pi$. We can make use of Equations 20 through 22 to find an expression for the allowed frequency of the TM_{npj} mode in a cavity of radius b and length L:

$$\omega_{npj} = \frac{1}{\sqrt{\mu\epsilon}}\sqrt{\left(\frac{z_{np}}{b}\right)^2 + \left(\frac{j\pi}{L}\right)^2}. \tag{29}$$

It would appear that, by applying conducting boundary conditions in the longitudinal degree of freedom, we at last have created a time-dependent electric field which is useful for acceleration of particles. By inspection if Equation 27, we can write a general solution to the time-dependent fields in a TM_{npj} mode:

$$
\begin{aligned}
E_z &= J_n(k_{c,np}r)\cos(n\theta)\cos(k_j z)\exp(i\omega t), \tag{30}\\
H_z &= 0,\\
E_r &= \frac{-k_j}{k_{c,np}}J_n'(k_{c,np}r)\cos(n\theta)\sin(k_j z)\exp(i\omega t),\\
E_\theta &= \frac{-k_j n}{k_{c,np}^2 r}J_n(k_{c,np}r)\sin(n\theta)\sin(k_j z)\exp(i\omega t),\\
H_r &= \frac{-i\omega\epsilon n}{k_{c,np}^2 r}J_n(k_{c,np}r)\sin(n\theta)\cos(k_j z)\exp(i\omega t),\\
H_\theta &= \frac{-i\omega\epsilon}{k_{c,np}}J_n'(k_{c,np}r)\cos(n\theta)\cos(k_j z)\exp(i\omega t),
\end{aligned}
$$

where $k_j \equiv j\pi/L$. As advertised, the E_r and E_θ components are zero at the endcaps; H_z is zero everywhere, including at the endcaps; and the partial derivatives of H_r and H_θ in the z direction are also zero.

Finally, let us consider the series expansion of $J_n(\mathcal{R})$:

$$J_n(\mathcal{R}) = \sum_{m=0}^{\infty} \frac{(-1)^m(\mathcal{R}/2)^{2m+n}}{m!(m+n)!}. \tag{31}$$

This expansion indicates that only the $n = 0$ modes will permit a longitudinal electric field on the axis of the cavity. This makes the $n = 0$ modes the preferred ones for actual acceleration. The cavity also needs a hole to let the beam through, but we'll discuss that detail shortly!

3.1 Transit Time Effect

Let us consider once again the (unacceptable) traveling wave mode TM$_{0p}$. We can express the electric field on axis as simply:

$$E_{z,0p} = E_0 \exp[i(\omega t - kz)], \tag{32}$$

where ω and k are understood to be non-negative. What is the energy gain received by the beam when it interacts with this wave over a distance L? If the beam is moving at the speed of light, then we can write $t = t_0 + z/c$, and express the energy gain edV in a distance dz,

$$edV = eE_{z,0p}dz = eE_0 \exp[i\omega t_0 + i\omega z/c - ikz]dz, \tag{33}$$

and integrate from $z = 0$ to $z = L$:

$$eV = eE_0 \Re \left\{ \exp(i\omega t_0) \int_0^L dz \exp[i(\omega/c - k)z] \right\}, \tag{34}$$

where we have explicitly required that only the real portion of our heretofore complex quantities can effect any meaningful changes on particles in the real world. Equation 34 can be evaluated:

$$eV = eE_0 \Re \left\{ \exp(i\omega t_0) \frac{\exp[iL(\omega/c - k)] - 1}{i(\omega/c - k)} \right\}. \tag{35}$$

The quantity $\psi \equiv L(\omega/c - k)$ is known as the *transit angle*, and represents the amount that the relative phase between the RF and the beam varies during the passage of the particles. We can rewrite Equation 35:

$$eV = eE_0 \Re \left\{ \exp(i\omega t_0) \frac{\exp(i\psi) - 1}{i\psi/L} \right\}. \tag{36}$$

Equation 36 can be written in an even-more useful form by: first, converting the $1/L$ in the denominator to a factor of L outside the brackets; second, factoring $\exp i\psi/2$ out of the numerator; and third, recognizing that the resulting expression has a startling resemblance to the expression for $\sin \psi/2$:

$$eV = eE_0 LT\Re \left\{ \exp[i(\omega t_0 + \psi/2)] \right\}, \text{ where} \tag{37}$$
$$T \equiv \frac{\sin(\psi/2)}{\psi/2}.$$

Equation 37 has a number of fascinating properties. First, it shows that the energy gain of passing particles is maximized when t_0 is selected such that $\omega t_0 + \psi/2$ is zero – in other words, the electric field experienced by the beam should achieve a maximum when the particle has travelled a distance $L/2$ from its starting point. Second, even if this optimum value is chosen, the energy gain of the particle will be reduced by a factor of T from what would be achieved if a DC field of E_0 was used for acceleration. Thus, the "efficiency" of acceleration (relative to a DC field) is maximized by minimizing the transit angle.

We can use Equation 37 to calculate the energy gain from a TM$_{0pj}$ mode in a cylindrical cavity. Recall that such a mode is composed of a left-travelling wave and a right-travelling wave superimposed within the cavity. Thus,

$$eV = e\frac{E_0 L}{2} \left\{ T_L \cos(\omega t_0 + \psi_L/2) + T_R \cos(\omega t_0 + \psi_R/2) \right\}, \tag{38}$$

where ψ_L and ψ_R represent the transit angle for leftward- and rightward-travelling waves, T_L and T_R their respective transit angle factors, and we have replaced the real portion of the complex

exponential with a cosine function. We can express the transit angles ψ_L, ψ_R as functions of the wave number k_j:

$$\psi_{L,R} = L\left(\frac{\omega}{c} \pm k_j\right), \tag{39}$$

where the $+$ sign corresponds to leftward-travelling and the $-$ sign to rightward travelling. We can combine our expression for $k_j = j\pi/L$ with the expression for ω_{npj} in Equation 29 to expand the transit angles:

$$\psi_{L,R} = \frac{1}{c\sqrt{\mu\epsilon}}\sqrt{\left(\frac{z_{0p}L}{b}\right)^2 + (j\pi)^2} \pm j\pi. \tag{40}$$

From Equation 40, we can see that, for leftward-travelling waves, the transit angle will be $2j\pi$ plus $z_{0p}L/b$ added in quadrature. For most combinations of parameters, this will give a negative value for $\sin(\psi_L/2)$ – that is to say, a decelerating wave. Apparently, if we want both the leftward- and rightward-travelling waves to contribute to the acceleration, the best mode choice is $j = 0$, corresponding to a standing wave with no longitudinal dependence (since the latter goes as $\cos(k_j z)$, and $k_{j=0} = 0$). Note that, for this solution, $\psi_L = \psi_R$, and the two cosine terms in Equation 38 can be maximized simultaneously by an appropriate choice of t_0. We can replace $\omega t_0 + \psi_{L,R}$ with a single phase offset and write the energy gain for a TM_{0p0} mode as:

$$\begin{aligned}
eV &= eE_0 LT\cos\phi, \text{ where} \tag{41}\\
T &= \frac{\sin(\psi/2)}{\psi/2}, \text{ and}\\
\psi &= \frac{L\omega}{c}.
\end{aligned}$$

3.2   R/Q

In order to maintain an accelerating field in the cavity, it will be necessary to store electromagnetic energy in the cavity. Since that energy ultimately comes from the electrical grid and has to be paid for, a useful quantity to calculate is the net acceleration achieved for a given quantity of stored energy. The energy density $\mathcal{U}$ is given by [3, 4]:

$$\mathcal{U} = \frac{1}{2}\left(\vec{E}\cdot\vec{D}^* + \vec{B}\cdot\vec{H}^*\right). \tag{42}$$

For a TM_{0p0} mode, only E_z and H_θ exist, and we can write:

$$\begin{aligned}
\vec{E}\cdot\vec{D}^* &= \epsilon\left[E_0 J_0(k_{c,0p}r)\right]^2\cos^2\omega t, \tag{43}\\
\vec{B}\cdot\vec{H}^* &= \mu\left[\frac{\omega\epsilon E_0}{k_{c,0p}}J_0'(k_{c,0p}r)\right]^2\sin^2\omega t.
\end{aligned}$$

If we select $t = 0$, Equation 43 requires that the magnetic energy density be zero throughout the cavity and we can compute the total stored energy using only the electric field components. Since total energy is conserved, and the E and H components in Equation 43 are out of phase with one another, one can see that the total stored energy in the cavity is oscillating back and forth between a purely-magnetic state and a purely-electric state.

we now wish to evaluate the total stored energy:

$$U = \frac{\epsilon}{2}E_0^2\int_0^b dr \int_0^L dz \int_0^{2\pi} r\,d\theta\, J_0^2(k_{c,0p}r). \tag{44}$$

14

The longitudinal and angular components can be evaluated by inspection, and one is left with a radial integration:

$$U = \pi \epsilon E_0^2 L \int_0^b r dr J_0^2(k_{c,0p}r). \tag{45}$$

We can simplify Equation 45 by introducing dimensionless variable $\mathcal{R} \equiv r/b$:

$$U = \pi \epsilon E_0^2 b^2 L \int_0^1 \mathcal{R} d\mathcal{R} J_0^2(z_{0p}\mathcal{R}). \tag{46}$$

Finally, we can use the fact that $\int_0^1 \mathcal{R} d\mathcal{R} J_0^2(z_{0p}\mathcal{R}) = J_1^2(z_{0p})/2$ [5]:

$$U = \frac{\pi}{2} \epsilon E_0^2 b^2 L J_1^2(z_{0p}). \tag{47}$$

Since $U \propto E_0^2$, we can sensibly form the ratio of the square of the effective accelerating voltage, $V^2 = (E_0 L T)^2$, to the stored energy required to achieve that acceleration:

$$\frac{V^2}{U} = \frac{2E_0^2 L^2 T^2}{\pi \epsilon E_0^2 b^2 L J_1^2(z_{0p})} \tag{48}$$

$$= \frac{2T^2}{\pi \epsilon J_1^2(z_{0p})} \frac{L}{b^2}.$$

Equation 48 can be usefully transformed by replacing one of the factors of b with $z_{0p}/(\omega_{0p0}\sqrt{\mu\epsilon})$, and moving the resulting factor of ω_{0p0} to the LHS:

$$\frac{V^2}{\omega_{0p0}U} = \frac{2T^2}{\pi z_{0p} J_1^2(z_{0p})} \frac{L}{b} \sqrt{\frac{\mu}{\epsilon}}. \tag{49}$$

The quantity $\sqrt{\mu/\epsilon}$ is the impedance of the medium, with units of ohms in MKSA, and is usually abbreviated Z, thus:

$$\frac{V^2}{\omega_{0p0}U} = \frac{2}{\pi z_{0p} J_1^2(z_{0p})} \frac{T^2 L}{b} Z. \tag{50}$$

We can make one additional simplification by noting that the term $2/[\pi z_{0p} J_1^2(z_{0p})]$ is equal to 0.982 for $p = 1$ and asymptotically approaches 1 for larger p values [6]. Thus, to excellent approximation, we can state that:

$$\frac{V^2}{\omega_{0p0}U} = \frac{T^2 L}{b} Z. \tag{51}$$

The quantity $V^2/(\omega_{0p0}U)$ is generally known as R/Q (read "R over Q" or "R upon Q"), for reasons which will be discussed later. Although it is referred to as the ratio of two quantities, R/Q is actually a purely geometric quantity of a given accelerating cavity, and it relates the resonant frequency, the achievable acceleration, and the stored energy which is required for operation.

We can improve the form of Equation 51 by noting that $T^2 = \sin^2(\psi/2)/(\psi^2/4)$ contains 2 factors of $1/L^2$ (in the $1/(\psi^2/4)$ component), thus:

$$\frac{R}{Q} = Z \frac{L}{b} \frac{\sin^2(\psi/2)}{\psi/2} \frac{2c}{L\omega_{0p0}}. \tag{52}$$

Recalling that $b = z_{0p}/\omega_{0p0}\sqrt{\mu\epsilon}$, we find:

$$\frac{R}{Q} = Z \frac{2}{z_{0p}} \frac{\sin^2(\psi/2)}{\psi/2} c\sqrt{\mu\epsilon}. \tag{53}$$

15

Equation 53 shows that the accelerating efficiency of a cavity is maximized when the $p = 1$ mode is used, since z_{0p} monotonically increases with p. It also shows that there is an optimum transit angle, since $\psi = 0$ results in a zero R/Q, and $\psi = 2\pi$ also yields zero R/Q. The maximum value of R/Q occurs at a transit angle of roughly $3\pi/4$ (actually, $133.56°$); at this angle, $\sin^2(\psi/2)/\psi/2 = 0.725$. R/Q is a relatively weak function of the transit angle: angles from $90°$ to $180°$ will yield values that are within 12% of the maximum value. Finally, we note that for a right circular cylindrical cavity, R/Q can be expressed as a function of transit angle alone, without any other dimensions or free parameters entering. Considering the definition of R/Q, one therefore surmises that accelerating voltage per unit of energy is optimized by maximizing the accelerating frequency and optimizing the transit angle.

In a real accelerating cavity, the value of R/Q will not be exactly the value given in Equation 53, since that relation does not include the effect of the hole through the cavity which lets the beam pass through. Even in a more realistic system, though, the principle of R/Q – that the relation between stored energy and voltage is a property of the cavity geometry alone, and that $V^2/\omega U$ is a constant for a given cavity – will remain true.

4 Multi-Celled Accelerating Cavities

In Section 3.2, we saw that the stored energy in a cavity is proportional to the square of the accelerating voltage in the cavity. Because of this, the most sensible approach to very high beam energies (such as 250 GeV, as proposed for the ILC) is the use of large numbers of cavities, rather than small numbers of cavities which are filled with a large energy density. By increasing the total number of cavities proportionally with the desired voltage, the total stored energy required is linearly proportional to the voltage rather than proportional to the square of the voltage. As we shall see, there are other practical limitations to RF acceleration, including the achievable gradient in a cavity; so distributing the acceleration over a large number of cavities, and reducing the voltage in each of the cavities, is a necessity.

One option for achieving large accelerations in a multi-cavity system is to have a large number of cavities which are each independently powered. This would require a large number of power sources (one per cavity), and a large number of waveguides which would transport power from the power sources to the cavities. Fortunately, this proves to be unnecessary. The necessary act of cutting a hole in each endcap of the cavity to allow the beam to pass through (!) will also allow us to solve the problem of providing power to each cavity.

4.1 Longitudinal Periodicity in Accelerating Structures

Consider a system shown in Figure 5: an infinitely long cylindrical waveguide with inner radius b contains a series of cylindrical plates which are evenly spaced a distance d apart in the guide; each plate has a thickness h, and each plate has a hole of radius a in the center. We assume that $a \ll b$, that $h \ll d$, and that the wall conductivity is infinite. We need to understand the electromagnetic fields which can be sustained in such a periodic structure.

In the limit of $a \to 0$, we expect the solution for the field in between each pair of plates to reduce to the single-cavity form which was determined in Section 3. We also know from Floquet's theorem that the infinite periodic system with holes will take a solution which satisfies [7]:

$$\vec{E}(r, \theta, z + d, t) = \vec{E}(r, \theta, z, t) \exp[d(-\alpha + ik_z)], \tag{54}$$

where α and k_z are real numbers and α is non-negative. A similar relation holds for $\vec{H}$.
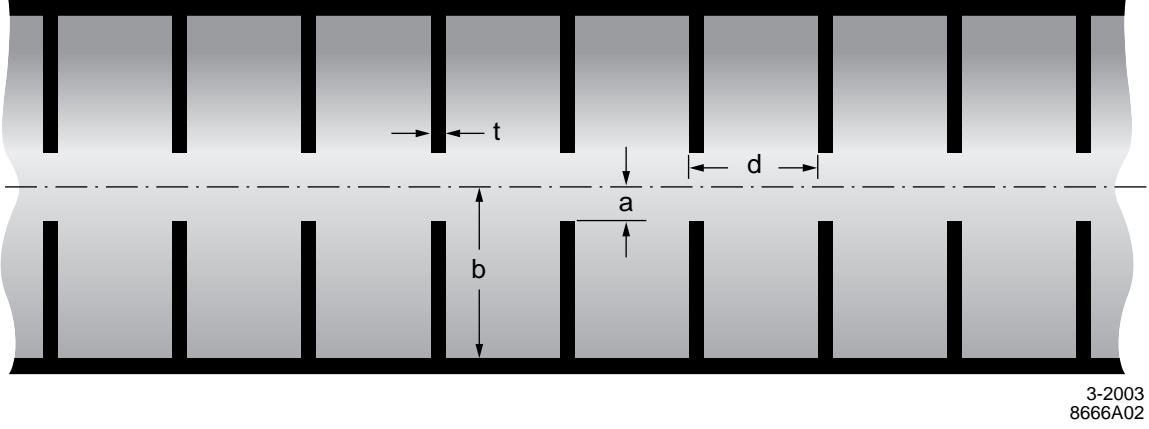
3-2003
8666A02

Figure 5: Longitudinal section of a cylindrical waveguide "loaded" with periodically-spaced discs.

Let us call the solution for the fields in the cavity in the absence of holes $\vec{E}_1, \vec{H}_1$, and the fields in the presence of the holes $\vec{E}_2, \vec{H}_2$, and consider the surface integral over the cavity's inner surface $\oint d\vec{A} \cdot (\vec{E}_1 \times \vec{H}_2^* - \vec{E}_2 \times \vec{H}_1^*)$[8], where $\vec{A}$ points *out* of the cavity. We can apply the divergence theorem to find:

$$\oint d\vec{A} \cdot (\vec{E}_1 \times \vec{H}_2^* - \vec{E}_2 \times \vec{H}_1^*) = \int d\text{Vol} \vec{\nabla} \cdot (\vec{E}_1 \times \vec{H}_2^* - \vec{E}_2 \times \vec{H}_1^*). \tag{55}$$

We can then apply a vector calculus identity to find:

$$\oint d\vec{A} \cdot (\vec{E}_1 \times \vec{H}_2^* - \vec{E}_2 \times \vec{H}_1^*) = \int d\text{Vol}[\vec{H}_2^* \cdot (\vec{\nabla} \times \vec{E}_1) - \vec{E}_1 \cdot (\vec{\nabla} \times \vec{H}_2^*) + \vec{E}_2 \cdot (\vec{\nabla} \times \vec{H}_1^*) - \vec{H}_1^* \cdot (\vec{\nabla} \times \vec{E}_1)]. \tag{56}$$

The curl operators in the above equation will precipitate the usual combination of i, ω, μ, and ϵ but will convert the vector operations to dot products of $\vec{H}_1^* \cdot \vec{H}_2$, and related permutations. If we require that the perturbation be small, then we can say that $\vec{H}_1 \approx \vec{H}_2$ and $\vec{E}_1 \approx \vec{E}_2$. We can thus write:

$$\oint d\vec{A} \cdot (\vec{E}_1 \times \vec{H}_2^* - \vec{E}_2 \times \vec{H}_1^*) = i(\omega_2 - \omega_1) \int d\text{Vol}(\mu \vec{H}_1^* \cdot \vec{H}_1 + \epsilon \vec{E}_1^* \cdot \vec{E}_1). \tag{57}$$

The quantity on the RHS is simply twice the stored energy in the unperturbed cavity. Thus we can derive the change in resonant frequency of the cavities with the holes, as compared to the cavities without the holes:

$$\omega_2 - \omega_1 = \frac{-i \oint d\vec{A} \cdot (\vec{E}_1 \times \vec{H}_2^* - \vec{E}_2 \times \vec{H}_1^*)}{2U_1}. \tag{58}$$

By inspection, we can eliminate the first term on the RHS of Equation 58. This is because the integral is over the surface of the unperturbed cavity, and on that surface $\vec{E}_1$ is normal to the surface at all points; therefore, $d\vec{A} \cdot (\vec{E}_1 \times \vec{H}_2^*)$ must vanish for all points on the surface. Outside of the region of the hole between cavities, $\vec{E}_2 \approx \vec{E}_1$; since $\vec{E}_1$ is normal to the surface at all points, the second term of the RHS of Equation 58 must also vanish, except in the region of the hole between cavities. The quantity $\vec{H}_1$ is the unperturbed magnetic field of the TM_{010} mode, for which a solution exists. Thus, once the radial electric field component in the vicinity of the hole is determined, we can estimate the change in the TM_{010} frequency in the infinite multi-cavity accelerating structure.

17

4.1.1 Radial Electric Field at the Cavity Hole

The present problem is to determine the electric field in the hole between two resonant accelerating cavities. In the absence of the hole, the field would of course be zero within the conducting material between cavities, and the electric field in the left and right cavities would be related by Floquet's theorem: $E_R = E_L \exp[d(-\alpha + ik_z)]$; in both cavities, the field would be purely longitudinal. In the presence of the hole, we can require that the total solution be a superposition of the hole-free system and a system containing only a conducting sheet with a hole. In the latter system we specify that the longitudinal electric field should go to E_L at $z = -\infty$ and to E_R at $z = +\infty$.

This problem has been solved in excruciating detail by Jackson [9], and here we quote only the result

$$E_r = \frac{E_L - E_R}{\pi} \frac{r}{\sqrt{a^2 - r^2}}. \tag{59}$$

4.1.2 Computing the Frequency Shift

We can now solve for the frequency shift in Equation 58. For $E_{2,r}$ we can write $E_0(1 - \exp[d(-\alpha + ik_z)])J_0(k_c r)r/\sqrt{a^2 - r^2}$; for $H_{1,\theta}^*$ we can write $i\omega_1\epsilon/k_c E_0^* J_0'(k_c r)$; put it all together, and we find:

$$2U_1(\omega_2 - \omega_1) = i \oint d\vec{A} \cdot \vec{E}_2 \times \vec{H}_1^* \tag{60}$$

$$= -\frac{\epsilon\omega_1}{2\pi k_c} E_0 E_0^* \{1 - \exp[d(-\alpha + ik_z)]\} \int_0^a r^2 dr \int_0^{2\pi} d\theta \frac{J_0(k_c r)J_0'(k_c r)}{\sqrt{a^2 - r^2}},$$

where we have included the fact that, due to sinusoidal oscillations, $\vec{E}_2 \times \vec{H}_1^* = (E_2 H_1^*)/2$ if we define $\vec{E}_2 \equiv \hat{E}_2 E_2 \exp(i\omega t)$, etc. Without too much controversy we can require that E_0 be real, that only the real component of the RHS of Equation 60 be used, and we can at the same time perform the angular integral:

$$2U_1(\omega_2 - \omega_1) = -\frac{\epsilon\omega_1}{k_c} E_0^2 [1 - \exp(-\alpha d)\cos(k_z d)] \int_0^a dr \frac{r^2 J_0(k_c r)J_0'(k_c r)}{\sqrt{a^2 - r^2}}. \tag{61}$$

The solution to the horrendous integral in Equation 61 is shown in detail in Appendix D. Here we jump to the solution:

$$U_1(\omega_2 - \omega_1) = -\frac{\epsilon\omega_1}{k_c} E_0^2 [1 - \exp(-\alpha d)\cos(k_z d)] \left(-\frac{1}{3} k_c a^3\right). \tag{62}$$

Our expression for U_1, Equation 47, can be used to find:

$$\omega_2 - \omega_1 = \frac{2}{3\pi} \frac{z_{01}}{J_1^2(z_{01})} \frac{a^3}{b^3 d} \frac{1}{\sqrt{\mu\epsilon}} [1 - \exp(-\alpha d)\cos k_z d], \tag{63}$$

where we have included the fact that there are two holes in each cavity, and therefore the frequency shift is twice what was originally calculated for one hole.

We can make a more useful expression by replacing the exponential decay, $\exp(-\alpha d)$, with the amount of attenuation expected at frequency ω_1 when passing through a hole of radius a and length h. Assuming that the hole is small (so that ω_1 is well below cutoff), the exponential term becomes $\exp(-z_{01}h/a)$. Finally, since $\omega_1 = z_{01}/(b\sqrt{\mu\epsilon})$, we can write:

$$\omega = \frac{z_{01}}{b\sqrt{\mu\epsilon}} \left(1 + \frac{2}{3\pi J_1^2(z_{01})} \frac{a^3}{b^2 d} [1 - \exp(-z_{01}h/a)\cos k_z d]\right). \tag{64}$$

18

Because we have made so many approximations to arrive at this result, Equation 64 is not accurate enough to actually use for the detailed design of a multi-celled accelerating cavity. It can be used to estimate the lowest-order properties of such a cavity, but the final design requires much more accurate estimating techniques, such as electromagnetic solvers.

4.2 Properties of the Multi-Celled TM_{010} Solution

Equation 64 shows us that, in the multi-celled TM_{010} system, we have returned to having a spectrum of allowed frequencies which can be supported by the accelerating structure, similar to the spectrum which is supported by the TM_{01} mode of regular waveguide. In the case of the TM_{01} mode in regular waveguide, the spectrum is semi-infinite: all frequencies above the cutoff frequency of $z_{01}/(b\sqrt{\mu\epsilon})$ can propagate. The multi-celled TM_{010} mode, on the other hand, has a *pass band*: frequencies in the range

$$\frac{z_{01}}{b\sqrt{\mu\epsilon}}\left(1+\frac{2}{3\pi J_1^2(z_{01})}\frac{a^3}{b^2d}[1-\exp(-z_{01}h/a)]\right) \leq \omega \leq \frac{z_{01}}{b\sqrt{\mu\epsilon}}\left(1+\frac{2}{3\pi J_1^2(z_{01})}\frac{a^3}{b^2d}[1+\exp(-z_{01}h/a)]\right)$$

(65)

can be propagated, all other frequencies are evanescent. Furthermore, there is a relationship between the frequency and the cell-to-cell phase difference demanded by Floquet's theorem.

Let us use the Floquet theorem wave number, k_z, and the frequency ω, to calculate the phase velocity of the resulting solution in the accelerating structure:

$$v_{\mathrm{ph}} = \frac{\omega}{k_z} = \frac{z_{01}}{k_z b\sqrt{\mu\epsilon}}\left(1+\frac{2}{3\pi J_1^2(z_{01})}\frac{a^3}{b^2d}[1-\exp(-z_{01}h/a)\cos k_z d]\right).$$

(66)

We can also calculate the group velocity – the velocity of energy propagation – for the structure:

$$v_{\mathrm{gr}} = \frac{d\omega}{dk_z} = \frac{z_{01}}{b\sqrt{\mu\epsilon}}\frac{2}{3\pi J_1^2(z_{01})}\frac{a^3}{b^2}\exp(-z_{01}h/a)\sin k_z d.$$

(67)

To make this more concrete, let us consider a waveguide with an inner radius b of 10 cm, a spacing between discs d of 10 cm, and a hole radius a of 5 cm; assume that h is approximately zero. Figure 6 shows ω as a function of k for (a) a circular waveguide with no discs (b) a single cavity with endcaps but not holes (c) an infinitely long multi-cell structure with discs and holes. Also shown is the speed of light line. (Note: the present parameters do not satisfy the requirement that a be small compared to b and d and thus a perturbation; the larger value is more illustrative because the small-a behavior is preserved but in a way that plots better.) As Figure 6 shows, the line representing the speed of light crosses the $\omega - k_z$ curve of the multi-celled structure, implying that there exists a frequency for which the phase velocity in the structure is c, which is essential for particle acceleration. The intersection occurs at $k_z \approx 27.6$ m^{-1}, indicating a wavelength of 22.7 cm and a frequency of 1.33 GHz. The factor $k_z d$ is 0.88π, or $158°$; Equation 67 tells us that the group velocity is 6.3% of the speed of light.

4.2.1 Finite-Length Structures

Figure 6 implies that an accelerating structure will propagate TM_{010}-like waves of any frequency between the lower and upper cutoff frequencies. This is true in the limit of an infinitely-long accelerating structure, but not in the case of a structure with a finite number of cells.

For a finite number of cells N_{cell}, the structure acts like a set of N_{cell} coupled oscillators, each of which has a resonant frequency equal to the lower cutoff frequency. Such a system has a total
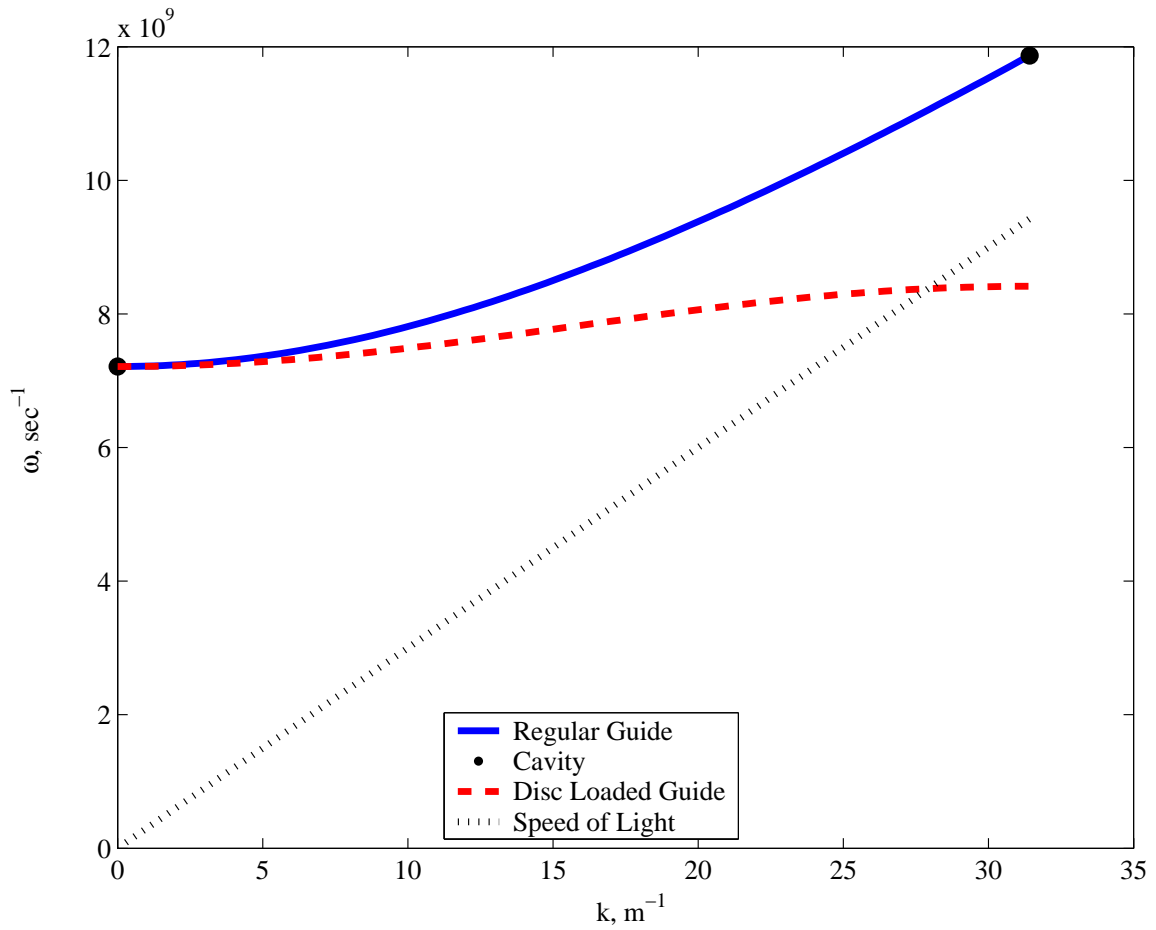
Figure 6: Diagram of ω vs k_z ("dispersion diagram") for regular waveguide, a single cavity with solid endcaps, and a disc-loaded waveguide. The line representing the speed of light is also shown.

20

of N_{cell} normal modes of oscillation; these modes are uniformly distributed in $k_z d$, from $k_z d = 0$ to $k_z d = \pi$, as shown in Figure 7. Because of the sinusoidal structure of the $\omega - k_z$ curve, the resonant frequencies are closely-spaced at the 0-mode and π-mode ends of the curve and more widely spaced in the center. In Figure 7, for example, the π-mode frequency is 1.373 GHz, while the $8\pi/9$-mode frequency is 1.366 GHz.

Why is this important? Note that the difference in frequency between the π-mode and the $8\pi/9$ mode is only 7 MHz out of 1.37 GHz, or about 0.5%. The phase velocities of the two modes are quite different, however: the former has a phase velocity of 0.92 c, while the latter has a phase velocity of 1.03 c, a difference of 10%. Were we to tune the parameters of the system to achieve a phase velocity of exactly c for the $8\pi/9$ mode, so that it would be ideal for accelerating ultra-relativistic electrons, then the phase velocity of the π-mode would be under 0.9 c. With a velocity difference between the beam and the RF of 0.1 c, the beam would slip from the "RF crest" (maximum acceleration) to the "RF trough" (maximum deceleration) over a distance travelled of about 1 meter, which is the total length of the RF structure (10 cells of 10 cm each). In short, if we tune the cavity in such a way as to make the $8\pi/9$ mode ideal for accelerating ultra-relativistic electrons, then the π mode will be useless. More generally, only the mode which is tuned to have a phase velocity of c is useful for the acceleration of ultra-relativistic electrons or positrons, and all other modes are useless.

Given all that, it is clear that the bandwidth of the system has to be small compared to the frequency separation between modes – if the RF source is off by 0.5%, for example, it will excite a useless mode rather than a useful mode. Similarly, there are practical limits to the number of cells that can be connected to form a single cavity, since the frequency separation between modes gets smaller as the number of cavities gets larger. At some point, the frequency separation between modes would be so small that the bandwidth requirements on the system as a whole would become impractically tight. We shall quantify "impractically tight" later...

4.2.2 Modes Other than TM$_{010}$

The analysis applied to the TM$_{010}$ mode, as extended to the multi-cell accelerating structure, can also be applied to the other modes that a single-cell cavity can support. Like the TM$_{010}$ mode, each cavity mode can be extended to a continuous spectrum of structure modes within a "pass band" of allowed frequencies; at each frequency there are an infinite number of modes with identical group velocities but varying phase velocities.

This has some rather interesting implications. Imagine that a structure which was built for linear acceleration is powered from a source which is at a frequency far above the TM$_{010}$ pass band. If the source frequency falls into the pass band of one of the other modes (TM$_{110}$ or TE$_{010}$, for example), then it will excite those modes. This allows accelerating structures to be used for purposes other than simple linear acceleration. Some examples include RF deflectors, which are accelerating structures operated at a frequency corresponding to a mode which includes a deflecting field at $r = 0$ – essentially, the device can be used as a steering element with a high-frequency, periodic deflecting field.

It is important to remember that any accelerating cavity has a rich spectrum of modes which can be excited, in addition to the operating mode that the user wants to excite. This will become important in our discussion on transverse and longitudinal wakefields later in this lecture and in the next one.
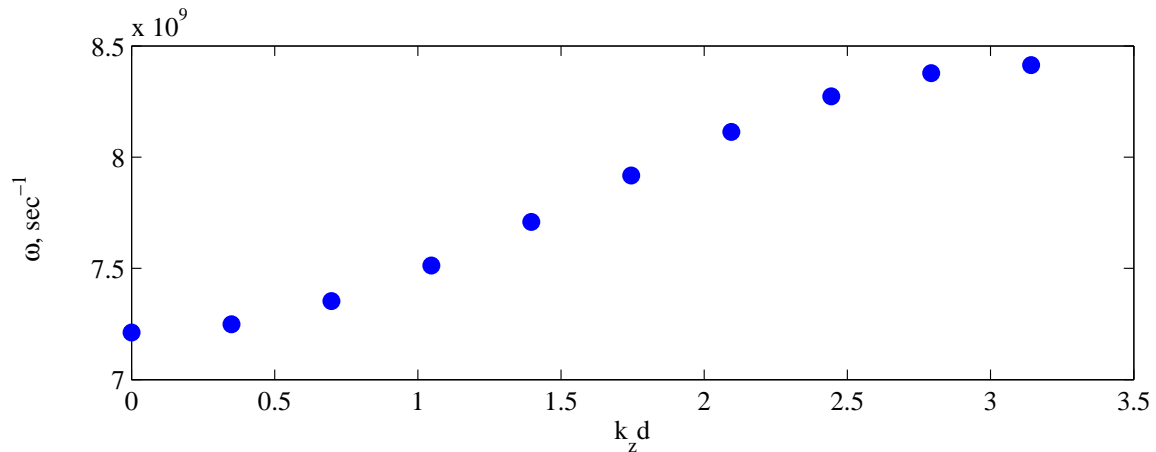
Figure 7: Normal modes of a disc-loaded waveguide with parameters identical to those used in Figure 6, but only 10 cells (rather than an infinite number of cells).

5 Accelerating Cavities with Finite Conductivity

So far we have assumed that the accelerating cavities are made from some material which has infinite conductivity (or, if you prefer, zero resistivity). What happens to an RF cavity if it is made from a material with a finite conductivity?

In the limit of infinite conductivity, we have seen in Equation 15 that RF electromagnetic fields are completely excluded from the material which forms the walls of the cavity. When the conductivity is very large but finite, this is no longer true: both electric and magnetic fields can now penetrate a short distance into the material of the cavity walls. The basic physics remains the same – the fields in the cavity are driving current flows in the walls which tend to cancel those fields at the transition from vacuum to the material of the cavity – but because of the finite conductivity, that cancelation occurs in a thin but finite layer of the wall, rather than a zero-thickness layer. This implies that, if the conductivity is high (so that the perfect-conductivity solutions are a good approximation to what really happens), then the fields in the material should be related in some way to the fields at the boundary in the infinite-conductivity case. In the interest of simplicity, we simply assert the result [10]

$$\vec{E}_c \approx \sqrt{\frac{\mu_c \omega}{2\sigma}} (-1 - i)(\hat{n} \times \vec{H}_s) \exp(-\xi/\delta) \exp(-i\xi/\delta), \tag{68}$$

where the subscript "c" refers to fields or permeability of the conductor, the subscript "s" refers to the field at the surface of the conductor, $\hat{n}$ is the normal vector pointing from the surface into the vacuum, ξ is a coordinate that points into the surface, and δ is the skin depth of the material at frequency ω:

$$\delta \equiv \sqrt{\frac{2}{\mu_c \omega \sigma}}. \tag{69}$$

Since the electric field in the material and the conductivity of the material are both finite, it follows that there will be energy dissipation in the skin of the material. The power dissipation per unit are can be computed by taking the electric field in Equation 68, multiplying by the current density (which is just $\sigma \vec{E}$), and integrating over ξ from the surface to infinite depth in the material.

22

A simple result can be obtained from this integration:

$$\frac{dP}{dA} = \frac{\mu_c \omega \delta}{2} |\vec{H}_s|^2 \tag{70}$$

We can use Equation 69 to eliminate the magnetic permeability of the cavity walls and the frequency of the RF, yielding:

$$\frac{dP}{dA} = R_s |\vec{H}_s|^2, \text{ where} \tag{71}$$

$$R_s \equiv \sqrt{\frac{\mu \omega}{2\sigma}} = \frac{1}{\sigma \delta}.$$

The quantity R_s is the "surface resistance" of the material, which is the surface resistivity divided by the skin depth.

5.1 Finite Conductivity and Superconducting Cavities

The accelerating cavities in the ILC are constructed from elemental niobium and operated at a temperature of about 2 K, well below the transition temperature to superconductivity (9.2 K for elemental niobium). The DC conductivity of elemental niobium under these conditions is as close to infinite as can be measured. In practice, however, the conductivity of the ILC accelerating cavities is finite due to two effects. First, the conductivity which is important to RF cavities is the AC conductivity, which is finite even for materials which are superconductors of direct current. Second, the niobium sheets which are used in the construction of RF cavities have impurities which cause even the DC conductivity of the resulting cavities to be finite. The impurities can be reduced, and the DC conductivity increased, but this increases the cost of the niobium material used in the accelerator.

5.1.1 AC Conductivity of Elemental Niobium

The physics issues which lead to a surface resistance for materials which are in a DC-superconducting state will be discussed in the SRF lectures. For now we simply state without proof or discussion the surface resistance [11]:

$$R_s[\Omega] \approx 9 \times 10^{-5} \frac{\nu^2[\text{GHz}]}{\mathcal{T}[\text{K}]} \exp\left(-\alpha_{sc}\frac{T_c}{\mathcal{T}}\right), \tag{72}$$

where $\mathcal{T}$ is the operating temperature, T_c is the critical temperature of 9.2 kelvin, and $\alpha_{sc} = 1.92$. Equation 72 shows that limiting the surface resistance of niobium cavities is accomplished by selecting a frequency and an operating temperature which are each as low as possible.

5.1.2 Residual Resistivity

The residual resistivity of a superconducting cavity is independent of temperature, depending mainly on impurities, imperfections in the crystalline lattice of the niobium, and so forth. As we shall see, it is practical to obtain niobium of sufficient purity that the residual resistivity is extremely small – residual surface resistance values of 3 nΩ can be readily achieved [12], and in this case the total surface resistance is dominated by the AC conductivity term described above. Another way of looking at this is that there is no point selecting parameters for an accelerating cavity such that the natural AC surface resistance is smaller than the expected surface resistance from impurities.

23

5.2 Accelerating Cavity Quality Factor

Let us now compute the power dissipation in a single-cell cavity operating in the TM_{010} mode, with length L and radius b. All that needs to be done is the integration of H_θ^2 over all of the surface. If we choose a time such that H_θ is maximized, then Equation 30 shows

$$|H_\theta| = E_0 \frac{\epsilon \omega_{010}}{k_{c,01}} J_0'(k_{c,01} r). \tag{73}$$

In the TM_{010} mode, $\omega_{010} = k_{c,01}/\sqrt{\mu\epsilon}$. Thus, we can eliminate the factor of $\epsilon\omega/k$ in Equation 73, and replace them with a factor of $1/Z$. We can calculate the total power loss in two integrals, one for the endcap and one for the barrel. The barrel integral can be performed almost by inspection:

$$
\begin{aligned}
P_{\text{barrel}} &= R_s \frac{E_0^2}{Z^2} \int_0^L dz \int_0^{2\pi} b d\theta [J_0'(k_{c,01} b)]^2 \tag{74} \\
&= \frac{2\pi E_0^2 R_s L b}{Z^2} [J_0'(z_{01})]^2 \\
&= \frac{2\pi E_0^2 R_s L b}{Z^2} J_1^2(z_{01}),
\end{aligned}
$$

making use of the J_0' identity from Appendix E. The endcap integral,

$$P_{\text{endcap}} = R_s \frac{E_0^2}{Z^2} \int_0^b r dr \int_0^{2\pi} d\theta [J_0'(k_{c,01} r)]^2, \tag{75}$$

can be solved with the use of the Bessel function identities from Appendix E to find the surprising result:

$$\int_0^b r dr [J_0'(z_{01} r/b)]^2 = \frac{b^2}{2} J_1^2(z_{01}). \tag{76}$$

Thus we can solve the endcap integral,

$$P_{\text{endcap}} = \frac{\pi E_0^2 R_s b^2}{Z^2} J_1^2(z_{01}). \tag{77}$$

We can put this all together, remembering that there are two endcaps and that the time-averaged power loss is $1/2$ of the losses calculated at the peak of the H-field, to find:

$$P_{\text{cav}} = \frac{\pi E_0^2 R_s}{Z^2} J_1^2(z_{01}) b(L + b). \tag{78}$$

Note that the effect of the beam hole in the single-cell cavity has been neglected in this calculation. The power dissipation in a multi-cell cavity is very nearly equal to the product of the dissipation in the single-cell cavity and the number of cells.

Equation 78 shows that the energy dissipation per unit time in the cavity walls is proportional to the square of the field amplitude in the cavity. Section 3.2 showed that the stored energy in the cavity is also proportional to the square of the field amplitude. This means that the dissipation of the stored energy in the cavity due to the resistance of the walls is an exponential decay process. The process is characterized by the ratio of the stored energy to the energy dissipated in 2π RF cycles, known as the cavity's quality factor or $\mathcal{Q}$. In this case, since we are considering only losses to the resistive walls, it is more specifically called, "Wall $\mathcal{Q}$":

$$\frac{\omega U}{P} = \frac{z_{01} Z L}{2 R_s (L + b)} \equiv Q_w. \tag{79}$$

Since $P \equiv dU/dt$, we can use Equation 79 to determine the time-evolution of the stored energy in the absence of an external power source:

$$U = U_{t=0} \exp(-\omega t/Q_w). \tag{80}$$

24

5.2.1 Quality Factor and Choice of Cell Phase Advance

Let us return to the 10 cell, 1 meter RF cavity describe in Sections 4.2 and 4.2.1. Assuming that we construct this structure of elemental niobium operated superconducting at 2 K, Equation 79 indicates that the wall $\mathcal{Q}$ will be 1.9×10^{10} (remember that L is the length of one cell, not the full length of the cavity). This means that the time needed for the stored energy in the cavity to decay due to wall losses is on the order of a second!

Now consider the group velocity of the $8\pi/9$ mode, which is the mode which has a phase velocity close to c. According to Equation 67, the group velocity is about 0.081 c. This means that RF power which is introduced at the upstream end of the cavity will reach the downstream end in 41.7 nanoseconds.

What happens to the RF power which reaches the downstream end of the cavity, 41.7 nanoseconds after being introduced at the upstream end? We have two options for what to do with it:

- Remove it from the cavity, or

- not.

If we inject RF power at the upstream end of the cavity and remove it at the downstream end, then we have a device which resembles the one pictured in Figure 8. Such a structure is usually called a "traveling-wave accelerator." Such accelerators have a long and honorable history in the annals of accelerator physics, but this is not a particularly good design for a superconducting accelerator. This is because the travel time for RF power is very short compared to the time needed for wall losses. In order to maintain a constant amount of stored energy in the cavity (and thus a constant accelerating field), the operator must continually supply power at the input coupler to make up the power which has propagated to the end and gone out via the output coupler. The biggest benefit of superconducting cavities – the fact that they can store energy for a very long time without significant wall losses – is completely lost because the RF energy is hardly being stored at all.

It should be noted that one way to make the design in Figure 8 work adequately in the superconducting limit is to connect the output coupler back to the input coupler and re-introduce the power which has left the cavity. Adding such a connection is a substantial design complication and not to be adopted without a very excellent reason!

The other design option is to replace the output coupler in Figure 8 with a piece of niobium, thus trapping the energy which has made its way to the downstream end of the cavity. The trapped energy will reflect off the end of the cavity and propagate back towards the upstream and the input coupler. This sounds like an improvement until we consider the fact that the reflection has a phase velocity of c but in the direction opposite of that of the beam! Since the beam and the reflected wave are (to put it mildly) not velocity-matched to one another, the reflected wave does not provide any net acceleration. Worse, the reflected wave doesn't stick around very long, either – 41.7 nanoseconds after reflecting off the downstream end of the cavity, the reflected RF power reaches the input coupler and exits the cavity entirely. In short, this is not in any way a better option than the two-coupler design.

From the preceding discussion, the root of the problem is clearly the very short transit time for RF power in the structure, which is a consequence of the very high group velocity of the $8\pi/9$ mode. The solution is therefore to design the structure to have a mode with a very low group velocity, and operate in that mode. As Equation 67 shows, the ideal solution is to operate in the π mode, which has a group velocity of zero, which means that the only time constant relevant to the operation of the cavity is the decay time for stored energy, which as we discussed is enormous.
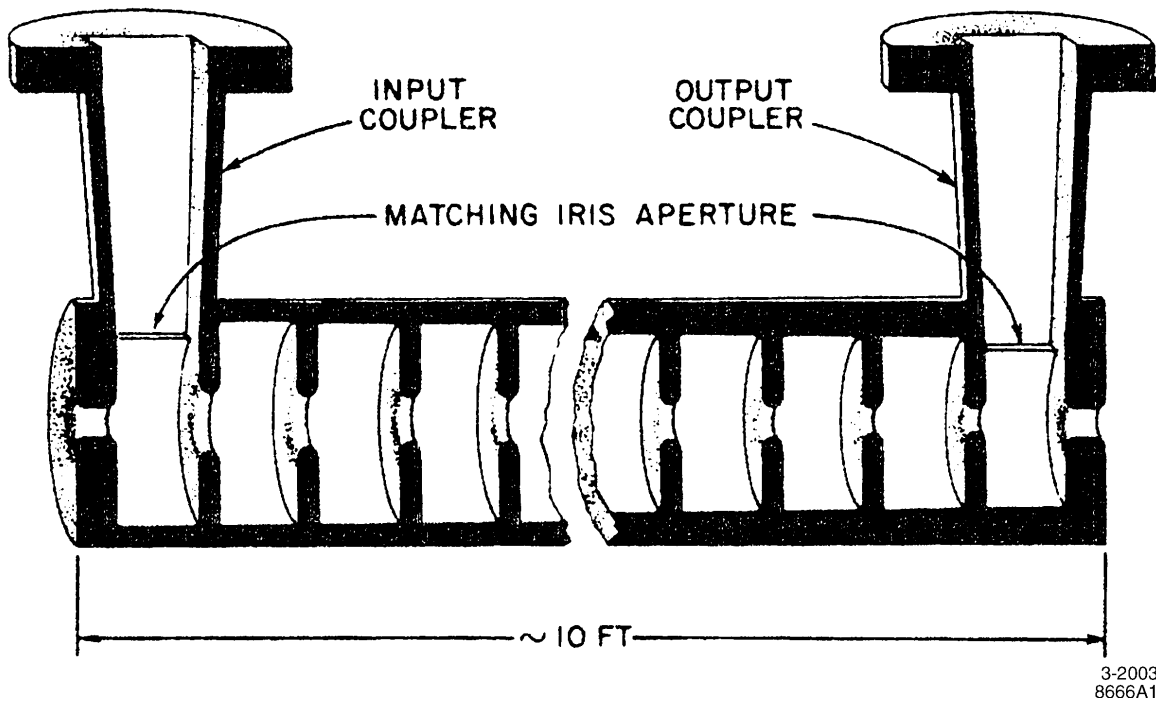
Figure 8: Schematic of a traveling-wave accelerator, in which RF power propagates from the input coupler to the output coupler through a series of cells.

Operating in a mode with zero group velocity would seem to introduce a serious problem of its own: how does the energy get from the input coupler cell to the other cells if the group velocity is really zero? One answer is, "don't worry about it" – for purposes of calculation, it is valid to take the approximation that the π mode is excited by the power supplied at the input coupler, that the excitation is uniform along the length of the cavity despite the apparent need for energy to propagate at speeds in excess of c, and that the standing-wave accelerator fills with energy "in time" while the traveling-wave accelerator fills "in space", as Loew and Neal put it [13]. This works for calculation but is intellectually unsatisfying.

To construct a more satisfying qualitative understanding of π mode operation, we must remember that each of the modes of the multi-cell cavity – from 0 mode to π mode and everything in between – is excited by the initial burst of RF energy into the empty cavity. We can see the time evolution of the cavity's response to the initial burst by constructing the superposition of all these excited modes. When we construct the superposition, we find that, as expected, the cavity which contains the input coupler is the first to fill with energy, and that neighboring cavities then fill from it. We also find that the acceleration seen by the beam due to this superposition of modes is exactly the same as the acceleration which would come from the π mode alone! In other words, in the time domain picture a particle which arrives in the cavity shortly after the first burst of RF energy is only accelerated in the coupler cell; but the acceleration it achieves in that cell is exactly what you would calculate considering only the π mode, and assuming that all the cells of the cavity are excited. The excitation from other modes causes the fields in the downstream cells to sum exactly to zero, and causes the fields in the excited cell to sum to exactly the level required to match the expected acceleration of the full π mode. Since the modes other than the π mode are driven far from their resonance frequency, they gradually decay away, leaving only the fields from

26

the desired π mode [14]. During this time, the different modes oscillate at different frequencies; in the time domain, the resulting time-dependent superposition results in the RF power traveling from one cell to another, but the acceleration seen by a beam passing through this ensemble of modes is always equal to the acceleration expected from the synchronous π mode alone[1] .

5.3 Shunt Impedance

Equation 79 shows that the wall $\mathcal{Q}$ is the ratio between the energy stored in a cavity, the power dissipated in the walls, and the frequency of the cavity. From Section 3.2, we have R/Q, which relates the cavity voltage to the stored energy and the frequency. We can combine these expressions to get a much more useful one, which is the relationship between the voltage in a cavity and the power dissipation in the walls:

$$R_{\text{cav}} = \frac{V^2}{P} = \frac{R}{Q}\mathcal{Q}. \tag{81}$$

The quantity R_{cav} has units of resistance, and so is known as the *shunt impedance* of the cavity. Equation 81 is amazingly useful in everyday life, since it allows us to treat the RF cavity like a resistor for purposes of calculation: given a shunt impedance R_{cav} and a desired voltage V, the required power is V^2/R_{cav}, just like in undergraduate electronics class! Note that there is a factor of 2 difference in convention between the resistor from undergraduate electronics and the RF cavity: for an AC voltage, the average power dissipated in the resistor is $V^2/2R$, whereas the factor of 2 is incorporated into the definition of shunt impedance for a cavity since we never deal with the dissipation of DC fields in RF cavities.

For a single-cell cavity with no beam holes, the expression for shunt impedance can be evaluated:

$$R_{\text{cav}} = \frac{Z^2}{R_s}\frac{2c^2\mu\epsilon}{z_{01}}\frac{\sin^2\psi/2}{1 + c\sqrt{\mu\epsilon}\frac{2}{z_{01}}\frac{\psi}{2}}, \tag{82}$$

where R_s is once again the surface resistance. Equation 82 has a maximum value of R_{cav} at $\psi = 158°$, but the maximum is broad enough that ψ values from 120° to 180° can be used with small (10% level) loss in efficiency.

For a multi-cell cavity, the shunt impedance of the whole is equal to the sum of the shunt impedances of the individual cavities. This, again, is similar to the lowly resistor encountered in undergraduate electronics class. One complication is that the ψ used to calculate the R_{cav} for one cell should be the distance from one face of the cell to the next, not the actual phase advance per cell (*ie*, leave out the portion of the cavity occupied by discs). In addition, there is a correction factor for the beam hole, which is empirically given by [15]:

$$R_{\text{cell}} \approx \frac{R_{\text{cav}}}{1 + 30.5(a/\lambda)^2}, \tag{83}$$

where R_{cav} is the single-cavity shunt impedance calculated without the correction for the hole, a is the radius of the hole, and λ is the RF wavelength. In the case of our hypothetical 10-cell structure, R_{cav} is extremely large – about $4.6 \times 10^{12}\Omega$ for one cavity, so 10 times that for the entire structure. On the other hand the very large hole in the cavity results in a large correction: Equation 83 shows that the shunt impedance is reduced to about 39% of this ideal value. The full 10-cell cavity has a shunt impedance of $1.78 \times 10^{13}\Omega$, and an R/Q of 771 Ω.

---

[1]Can one go further and model a traveling-wave structure as a series of stationary modes, and the apparent "traveling" of the RF power as a consequence of the different modes oscillating at different frequencies and driven off-resonance? Yes.

6   Introducing the RF Power

So far we have talked about multi-cell RF cavities with perfect rotational and translational symmetry – devices which are featureless except for the hole that the beam passes through. A real cavity needs to allow at least one more thing in, which is the RF power from an external source which provides the stored energy which creates the fields which leads to acceleration.

In order to introduce RF power, we need to cut a specialized hole in the RF cavity, known as an *RF coupler*. The coupler will allow some of the incident RF power to pass into the cavity, and will reflect the rest back towards the RF source. One might think that reflecting a lot of power back towards the source would be a Bad Thing (it is at least not very energy efficient), and so one should design a coupler which transmits most of the power into the cavity. Unfortunately, a coupler is a two-way passage: if it is very good at letting power into the cavity, it's also very good at letting power out of the cavity. Since the biggest benefit of a superconducting cavity is that it can store energy with very low losses for a very long time, having an RF coupler which allows all that stored energy to pour out defeats the purpose of going superconducting in the first place.

6.1   Time Evolution of the Stored Energy

To understand more fully the implications of this, we follow the approach of Nantista [16]: a monochromatic power source supplies a wave with amplitude E_{in}, which is incident upon a resonant cavity of some kind; the boundary between the cavity and the input waveguide is an iris with reflection coefficient Γ. In general Γ is real and negative, which causes a reflected wave which is out of phase with the incident wave, $E_{\text{ref}} = \Gamma E_{\text{in}} = -|\Gamma| E_{\text{in}}$. Meanwhile, there is also an electromagnetic wave, E_{e}, which is the wave emitted from the stored energy in the cavity (ie, the stored energy is "leaking out" through the iris). The net amplitude flowing backwards, from the iris towards the power source, is $E_{\text{out}} = E_{\text{e}} + \Gamma E_{\text{in}}$.

Now let us require that energy be conserved, which on an instantaneous basis means that RF power must also be conserved. The amount of power incident on the iris from the power source must be equal to the sum of the power in the reverse wave, the power lost in the walls of the resonant cavity, and the instantaneous increase in the stored energy in the cavity:

$$P_{\text{in}} = P_{\text{out}} + P_{\text{c}} + \frac{dU_{\text{c}}}{dt}. \tag{84}$$

Let us define the proportionality between the power in the waveguide and the resulting square of the field amplitude as $\mathcal{K}_{\text{wg}}$, such that $P_{\text{in}} = \mathcal{K}_{\text{wg}} E_{\text{in}}^2$, and similarly $P_{\text{out}} = \mathcal{K}_{\text{wg}}(E_{\text{e}} + \Gamma E_{\text{in}})^2$. In the absence of incoming power, obviously $P_{\text{out}} = \mathcal{K}_{\text{wg}} E_{\text{e}}^2$. From the definition of wall Q, Equation 79, we know that $P_{\text{c}} = \omega U_{\text{c}}/Q_w$. It can be shown that, in the absence of incoming power, the outgoing power is also proportional to the stored energy and thus to the power lost into the cavity walls. We can define the ratio of power emitted from the cavity to power lost in the walls as the cavity coupling coefficient, β_{c}:

$$\beta_{\text{c}} \equiv \frac{P_{\text{out}}}{P_{\text{c}}}, \ \ P_{\text{in}} = 0. \tag{85}$$

Putting all this together allows us to write:

$$U_{\text{c}} = \frac{Q_w}{\omega} P_{\text{c}} = \frac{Q_w}{\omega} \frac{\mathcal{K}_{\text{wg}} E_{\text{e}}^2}{\beta_{\text{c}}}. \tag{86}$$

Let us now recast Equation 84, with some substitutions:

$$\mathcal{K}_{\text{wg}} E_{\text{in}}^2 \ = \ \mathcal{K}_{\text{wg}}(E_{\text{e}} + \Gamma E_{\text{in}})^2 + \frac{\mathcal{K}_{\text{wg}}}{\beta_{\text{c}}} E_{\text{e}}^2 + \frac{2\mathcal{K}_{\text{wg}} Q_w}{\omega \beta_{\text{c}}} E_{\text{e}} \frac{dE_{\text{e}}}{dt}, \ \text{or} \tag{87}$$

$$E_{\text{in}}^2 = (E_\text{e} + \Gamma E_{\text{in}})^2 + \frac{1}{\beta_\text{c}} E_\text{e}^2 + \frac{2Q_w}{\omega \beta_\text{c}} E_\text{e} \frac{dE_\text{e}}{dt},$$

where we have taken the time derivative of Equation 86. If we assume, as discussed above, that $\Gamma \approx -1$, then we can write a simple differential equation which describes the emitted wave amplitude:

$$2E_{\text{in}} = E_\text{e} \left(1 + \frac{1}{\beta_\text{c}}\right) + \frac{2Q_w}{\omega \beta_\text{c}} \frac{dE_\text{e}}{dt}, \text{ or} \tag{88}$$

$$\frac{\omega \beta_\text{c}}{Q_w} E_{\text{in}} = \frac{dE_\text{e}}{dt} + E_\text{e} \frac{\omega}{2Q_L},$$

where $Q_L \equiv Q_w/(1 + \beta_\text{c})$ is called the *loaded* Q (ie, the Q – the proportionality between the RF period and the *e*-folding time – when the cavity is "loaded" by the coupler as well as the wall losses). If we define the characteristic time of the system, $t_\text{c} \equiv 2Q_L/\omega = 2Q_w/[\omega(1 + \beta_c)]$, then we can rewrite Equation 88 in an even-more compact and useful form:

$$t_\text{c} \frac{dE_\text{e}}{dt} + E_\text{e} = \frac{2\beta_\text{c}}{1 + \beta_\text{c}} E_{\text{in}}. \tag{89}$$

If we assume that $E_{\text{in}} = 0$ for $t < 0$ and is a constant for $t > 0$, we can solve Equation 89:

$$E_\text{e} = \frac{2\beta_\text{c}}{1 + \beta_\text{c}} E_{\text{in}} \left(1 - e^{-t/t_\text{c}}\right). \tag{90}$$

Similarly, we can now solve for $E_{\text{out}} = E_\text{e} - E_{\text{in}}$:

$$E_{\text{out}} = \frac{2\beta_\text{c}}{1 + \beta_\text{c}} E_{\text{in}} \left(1 - e^{-t/t_\text{c}}\right) - E_{\text{in}}. \tag{91}$$

Note that, for $\beta_\text{c} = 1$, the backwards-wave amplitude E_{out} goes asymptotically to zero, as the reflected and emitted waves become equal and opposite. The characteristic "e-folding" time for the cavity with input coupler is t_c, which is the filling time of a standing-wave cavity.

How do the stored energy and the accelerating voltage of a standing-wave structure vary with time? Equation 86 defines the stored energy as a function of the emitted wave amplitude, which we solved for in Equation 89. With appropriate simplifications,

$$U_\text{c}(t) = t_\text{c} P_{\text{in}} \frac{2\beta_\text{c}}{1 + \beta_\text{c}} \left(1 - e^{-t/t_\text{c}}\right)^2. \tag{92}$$

Similarly, by the definition of R/Q, we find:

$$V(t) = \left(1 - e^{-t/t_\text{c}}\right) \sqrt{\frac{R}{Q} \omega t_\text{c} P_{\text{in}} \frac{2\beta_\text{c}}{1 + \beta_\text{c}}}. \tag{93}$$

For superconducting RF structures, as we shall see, it is typical for $\beta_c \gg 1$, so that we can rewrite the stored energy and voltage expressions as:

$$U_c(t) \approx 2t_\text{c} P_{\text{in}} \left(1 - e^{-t/t_\text{c}}\right)^2, \quad V(t) = \left(1 - e^{-t/t_\text{c}}\right) \sqrt{2\frac{R}{Q}\omega t_\text{c} P_{\text{in}}}, \tag{94}$$

or,

$$U_c(t) \approx \frac{4Q_L}{\omega} P_{\text{in}} \left(1 - e^{-t/t_\text{c}}\right)^2, \quad V(t) = 2\left(1 - e^{-t/t_\text{c}}\right) \sqrt{\frac{R}{Q}Q_L P_{\text{in}}}. \tag{95}$$

29

From the definition of t_c, we see that reducing the loaded Q value decreases the amount of time it takes to fill a cavity, while from Equation 95 we see that it also decreases the maximum attainable voltage in the cavity. This makes sense, since the loaded Q is in some sense a measure of the "leakiness" of the input coupler.

To make this concrete, let us return to the example RF cavity from previous sections. In the interest of round numbers, let us tune the input coupler to give $Q_L = 10^6$, and use an input power of $P_{\text{in}} = 1$ MW. Using a π mode frequency of $\nu = 1.373$ GHz, the characteristic time t_c of the system is 232 microseconds. At equilibrium ($t \to \infty$), the cavity voltage will reach 55.5 MV. Figure 9 shows the time evolution of the emitted field, the total field going towards the RF power source, the stored energy, and the voltage in the cavity.

Since the loaded Q value is the one which is most important to the RF power dynamics of the cavity, why do we care as much as we do about the wall Q? After all, if the loaded Q is 3 orders of magnitude below the wall Q, as in the example above, it seems like we could construct the cavities to have a much lower wall Q, and lower cost, while maintaining the same loaded Q, gradient, etc. The answer is that the power lost into the walls is still determined by the wall Q, and this power is the power which must be extracted at 2 K – the power loss which is measured by the loaded Q is power which is sent to a room-temperature load. As we shall see in later lectures, removing heat from a 2 K system is an extremely inefficient process – typically the refrigeration system consumes 500-1000 watts for every watt which has to be removed at 2 K. Thus, it is important to build the system with the highest wall Q achievable, even if we are then going to load down the system to a much lower loaded Q with an input coupler.

What about the actual RF power which is directed away from the cavity and back towards the RF source? We can use the proportionality that at $E = E_\in$, the power is equal to 1 MW, and the fact that the power is proportional to E^2, and plot this quantity as well; the result is shown in Figure 10. At $t = 0$, the power transmitted back towards the source is the full 1 MW, as almost all the power gets reflected. As the cavity slowly fills, it emits fields which are out of phase with the reflected fields, causing the total power directed at the source to reduce; after some time, the emitted fields are larger than the reflected ones, so the total power increases again. At equilibrium, the power directed at the source will be only slightly below 1 MW. This is a typical result for $\beta_c \gg 1$ – at equilibrium, the power directed back towards the source equals the power from the source. Since energy is conserved, the power which actually passes through the input coupler into the cavity has the opposite behavior: at $t = 0$ and $t \to \infty$, zero power passes through the coupler, while at an intermediate time all of the RF power from the source flows through the coupler and into the cavity.

6.2 Handling the Reflected Power

Figure 10 shows that the amount of reflected and/or emitted power from the cavity is comparable to the power from the RF source itself. In the next section we will see that most of this power is absorbed by the beam, but not all of it. Since reflected power is bad for the health of a high-powered RF source, it is not acceptable to simply let that power return to the source. There are at least two ways to prevent this outcome.

6.2.1 Circulators

The first option is to redirect the backwards-propagating RF away from the source with a *circulator*. The circulator consist of ferrite material in a strong magnetic field parallel to the RF propagation; the magnetic field is generated by permanent magnets for energy efficiency. The circulator breaks
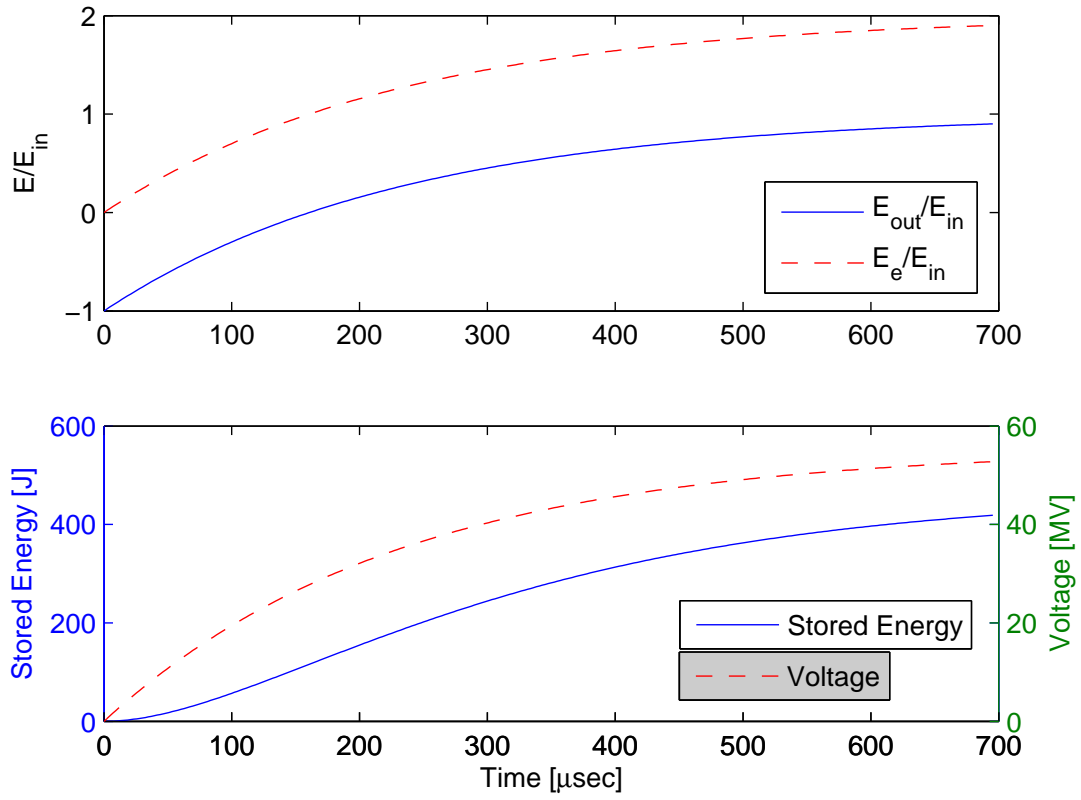
Figure 9: Time evolution of the emitted field and total field directed towards the RF source (top); stored energy and total voltage (bottom).
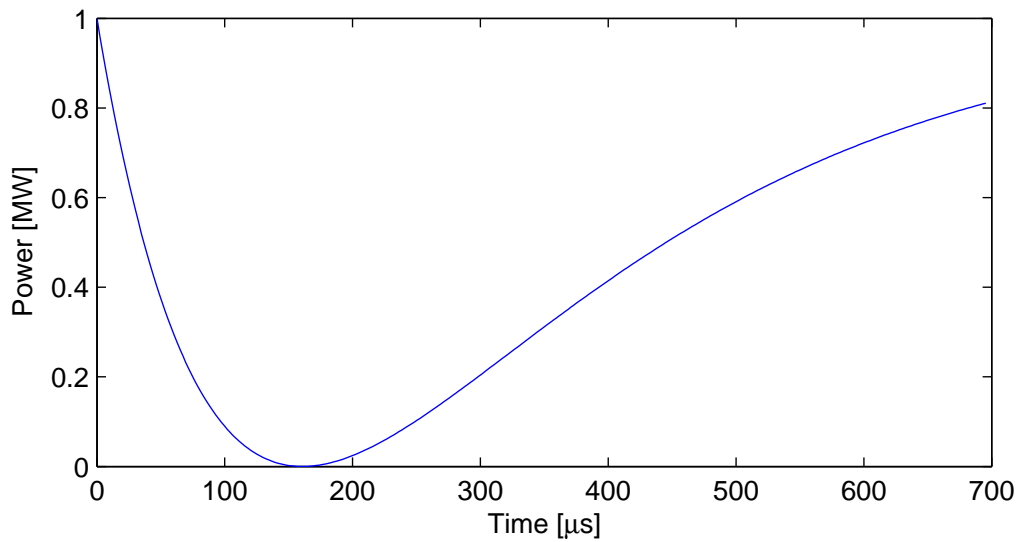

Figure 10: Time evolution of the power directed back towards the RF source from the coupler.

31

the forward-backward symmetry of the waveguide and allows backward-propagating waves to be directed away from the RF source and sent to a water-cooled load.

6.2.2 Magic Tee

A "magic tee" is a 4-port RF splitter/combiner. It is a passive device, which is constructed such that when one injects equal RF power into two of the ports (conventionally ports 2 and 3), all of the power goes into one port (port 1) if the inputs at ports 2 and 3 are in phase, and the other port (port 4) if the inputs at port 2 and 3 are $180°$ out of phase.

So how does this help? Imagine that the RF power source is located at port 1; ports 2 and 3 go to two different RF cavities; port 4 goes to a water-cooled load. If the path from the magic tee to the cavity at port 3 is 1/4 wavelength longer than the path from the tee to the cavity at port 2, then RF power from the source (at port 1) will be split equally and sent to ports 2 and 3; power going to the cavity at port 3 takes a longer path than power to port 2, and reflected power has the same added path length, so the reflected power which returns to the tee at port 3 has a $180°$ phase shift relative to reflected power which returns to the tee at port 2; so the reflected power from the two cavities is summed at port 4, the load, not port 1.

The magic tee solution has a few disadvantages relative to the circulator solution. The magic tee requires two cavities with a specific wavelength relationship between them, so that the reflected waves combine exactly and are directed at the load. If one of the cavities produces reflected energy but the other does not (for example, if the power or filling times of the cavities are mismatched, or there is some other problem which causes mismatched reflections), then the mismatched reflected power splits between the load and the RF source, whereas a circulator would always direct all the power away from the RF source. The major advantage of the magic tee is that it is an inexpensive, simple device compared to the circulator.

7 Introducing the Beam

So far we have talked about the RF cavity in isolation, as a device which can be filled with energy in order to produce a longitudinal electric field. What we really want to do, of course, is apply that longitudinal electric field to a beam!

Let us consider a beam with a steady-state current I_{beam}, with a time structure of bunches with a uniform charge per bunch q and an inter-bunch interval $t_b \equiv q/I_{\text{beam}}$ (this is usually known as a *bunch train*); and let us assume that the RMS bunch length σ_z is very small compared to the RF wavelength λ. The beam also has a duty factor H: in other words, the current in the accelerator is I_{beam} only for a small fraction of the time, given by H, and is zero for a fraction of time $1 - H$. We intend to accelerate the beam in a cavity with voltage V; this will result in an increase in the energy of each bunch given by qV, and a transfer of power to the beam of $I_{\text{beam}}V$. Our requirements on the acceleration of the beam are the following:

- We want to provide *the same acceleration* to every bunch in the bunch train – a high acceleration for early bunches and a low acceleration for late bunches (or vice versa) are not acceptable.

- We want to keep the RMS energy spread within each bunch as low as possible.

- We want to maximize the energy efficiency of the acceleration process, since ultimately we have to pay for every joule of electrical energy that we use from the power grid.

How do we go about putting these requirements into practice?

7.1 Steady-State Beam Loading

From Equation 95, we see that the cavity voltage is not a constant, but evolves in time according to $1 - e^{-t/t_c}$; thus, it would appear that only at $t = \infty$ can we achieve a uniform accelerating voltage for the beam, and infinity seems like a long time to wait before injecting the first bunch train.

Fortunately for us, introducing the beam changes the dynamics of the RF cavity, and it does so by absorbing some of the stored energy in the cavity. This in turn reduces the voltage in the cavity. We can achieve a uniform accelerating voltage, then, by making the beam-induced reduction in cavity voltage match the increase in cavity voltage caused by the incoming RF power.

More concretely, we see from Equation 95 and Figure 10 that the voltage is increasing because the stored energy in the cavity is increasing, and the stored energy in the cavity is increasing because the portion of RF power which is not reflected towards the RF source is entering the cavity. We can achieve a voltage which is fixed in time by selecting a beam current such that at the desired voltage V_0, $I_{\text{beam}} V_0 = P_c$ – that is, the product of the desired voltage and the beam current exactly equals the power into the cavity at the desired voltage. Since the beam absorbs all of the power which is entering the cavity, the stored energy in the cavity becomes fixed in time, leading to a voltage which is also fixed in time.

From Figure 10, we can see that the power transmitted to the cavity varies from zero at $t = 0$ and $t \to \infty$, to the full power of the RF source P_{in} at some intermediate time; and that all the power which does not go into the cavity is reflected back towards the RF source and ultimately dumped in a water-cooled load. Since the power which is dumped in the load is wasted, our requirement for efficient acceleration naturally leads us to want to operate under the condition where all of the power is going into the cavity and none of it is going into the load. From Equation 91, we can see that the moment when the power to the cavity is maximized occurs when $e^{-t/t_c} = 1/2$, or $t = t_c \ln 2$. From Equation 95, we can see that at that moment, the cavity voltage is exactly half of the voltage it would achieve at $t \to \infty$ in the absence of the beam: $V_0 = \sqrt{Q_L P_{\text{in}} R/Q}$.

7.1.1 Selection of Parameters

More generally, we see that we have four parameters which need to be specified: V_0, I_{beam}, P_{in}, Q_L. Two of these are free parameters, which we can specify, and typically V_0 and I_{beam} are the ones we choose. The other parameters, P_{in} and Q_L, are determined by the requirement that:

$$V_0 = \sqrt{Q_L P_{\text{in}} \frac{R}{Q}}, \tag{96}$$

$$I_{\text{beam}} V_0 = P_{\text{in}}.$$

We can use Equation 96 to find the requirement on the loaded Q value,

$$Q_L = \frac{V_0}{I_{\text{beam}} \frac{R}{Q}}. \tag{97}$$

In the case of our sample cavity, of course, we chose $Q_L = 10^6$ and $P_{\text{in}}=1$ MW for the convenience of the numbers, so we have to do the reverse: find the voltage V_0 and the current I_{beam} from the Q_L and P_{in} values. In this case, we find $V_0 = 27.8$ MV, $I_{\text{beam}} = 36$ mA.

7.1.2 Life Cycle of an RF Pulse

With the parameter selection in hand, we can now describe the life cycle of an RF pulse:
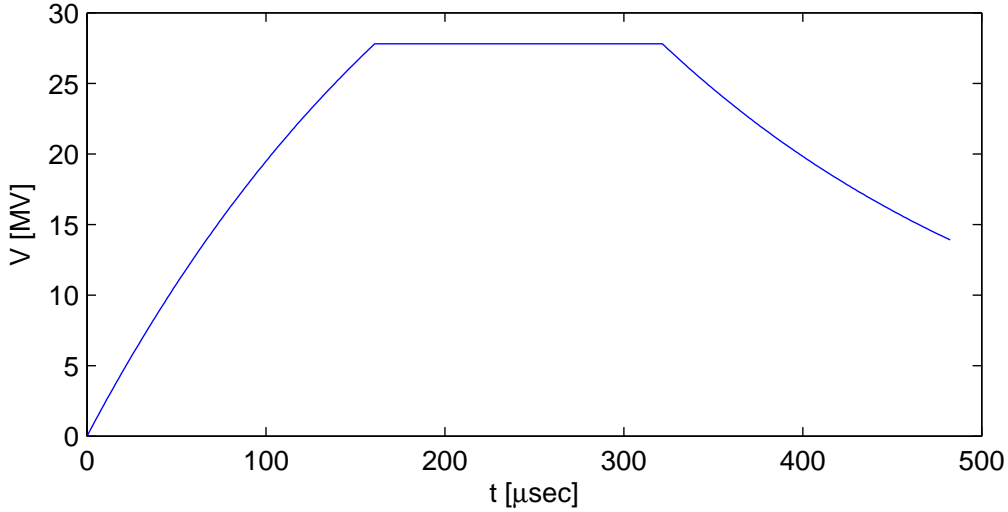
Figure 11: Life cycle of an RF pulse in the case of our example RF cavity.

- From $t = 0$ to $t = t_1 \equiv t_c \ln 2$, the power from the RF source P_{in} fills the RF cavity, and the voltage and stored energy evolve as shown in Equation 95; no beam is present during this time. At $t = t_1$, the voltage in the cavity is V_0, which is exactly $1/2$ of $V(t \to \infty)$.

- At $t = t_1$, the beam with current I_{beam} is introduced. The stored energy in the cavity is now fixed, since the beam absorbs all of the power coming from the source, and the voltage is fixed at V_0.

- At a later time t_2, both the beam and the RF source are turned off. At this point the power and voltage both decay, the latter decays as $V = V_0 e^{(t-t_2)/t_c}$.

- After a time $(t_2 - t_1)/H$, the whole process repeats itself.

Figure 11 shows the time evolution of the cavity voltage for our example RF structure, with $t_c = 232$ μsec and V_0=27.8 MV. In this case we have chosen $t_2 = 2t_1$ for convenience of plotting, and have truncated the exponential decay of the voltage after $3t_1$, again for convenience. We have also taken the approximation of a constant, uniform beam current. In actuality, of course, the beam has bunches with a bunch interval between them: what actually happens is that the voltage becomes a small "sawtooth" rather than a "flat-top", with each bunch causing the voltage to step down and the input power between one bunch and the next causing the voltage to rise back to V_0.

7.1.3   Beam-Induced Fields

As Wangler points out [19], the beam is more than just a medium that absorbs RF power from the cavity and acts like a resistive load, but it is in fact a source of fields in the cavity as well[2].In order to see this, consider a cavity with no power source which has a beam passing through it. The beam is composed of bunches which are here assumed to be infinitely short, but any bunch length $\sigma_z \ll \lambda$ would be acceptable. Because each bunch is charged and ultra-relativistic, it is accompanied by a "pancake" of electromagnetic fields; because the bunch is infinitely short, the spectrum of the

---

[2]I liked Wangler's formulation of this so much that I have used it, almost word-for-word, here.

bunch (which is the Fourier transform of its length) is infinitely wide. This means that there is a component of the bunch's field which is at the resonant frequency of the RF cavity. When the bunch passes through the cavity, the component of its field which is at the cavity frequency acts just like an RF power source and excites the cavity. The implication is clear: the passage of the bunch causes some electromagnetic energy to be stored in the cavity; and that means that the bunch must decelerate, since energy is conserved and the stored energy of the cavity has just increased.

How can we compute the amplitude of the beam-induced fields on this unpowered cavity? The simplest way to do this is to note that we have already computed the amplitude of the fields in a cavity which had an active RF power source but no beam, and the amplitude of the fields in a cavity which had both an active RF power source and a beam. This last case must be a superposition of the fields from the RF and the fields from the beam; so the fields from the beam must be the difference between the fields with both beam and RF and with RF but no beam.

In Figure 12, we return to the example of our beam-loaded cavity, but in this case we plot both the loaded and the unloaded voltages. The difference between these must be the beam-induced field. Note that, since the unloaded cavity voltage adiabatically approaches twice the loaded voltage, it must be the case that the voltage from beam loading adiabatically approaches the loaded voltage as well. In other words, if your cavity was supplying an accelerating voltage V_0 when powered, it will supply a decelerating voltage V_0 when unpowered but beam loaded.
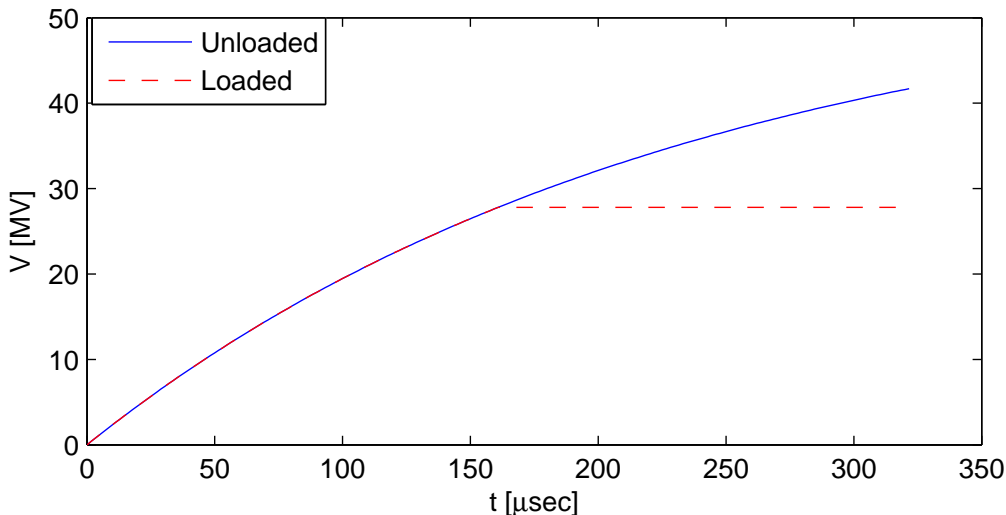

Figure 12: Unloaded (blue,solid) and beam-loaded (red, dashed) voltages in the case of our example RF cavity.

In the steady state, the beam current I_{beam} is decelerated by a voltage V_0, so the steady-state power removed from the beam is $I_{\text{beam}}V_0$; we also know that, in order to sustain a steady-state voltage of V_0, the power required is given by $V_0 = \sqrt{Q_L PR/Q}$. Setting these two power terms equal, we find that at steady-state,

$$V_{\text{beam}} = -I_{\text{beam}}Q_L\frac{R}{Q}. \tag{98}$$

Furthermore, since the voltage slope from loading can exactly cancel the voltage slope from the RF power source, it follows that they must both have the same exponential behavior. This leads us to

35

an expression for the beam loading voltage as a function of time:

$$V_{\text{beam}}(t) = -(1 - e(t - t_1)/t_c)I_{\text{beam}}Q_L\frac{R}{Q}, \ t \geq t_1 \tag{99}$$
$$= 0, \ t < t_1.$$

7.1.4 Off-Crest Running

So far we have implicitly assumed that the beam is being accelerated at the RF crest. This is obviously desirable in the linac, since it maximizes the energy efficiency of the acceleration, but it is not always possible. For example, in the bunch compressor, it is necessary to run the beam through the RF almost at the zero-crossing of the RF, since what is desired is not to accelerate the beam but to induce the dE/dz which is needed to achieve compression. In the linac, it is often desirable to have extra accelerating voltage available to compensate for slow variation in the overall voltage or to compensate for RF stations which have unexpectedly stopped working: this often requires additional RF stations which operate far from the RF crest normally, but which move closer to on-crest operation when additional "make up" voltage is needed. Assuming a phase angle ϕ between the beam and the RF, the resulting mean acceleration of the beam is given by:

$$V = V_{\text{unload}} \cos \phi + V_{\text{beam}} \tag{100}$$
$$= 2(1 - e^{-t/t_c})\sqrt{Q_L P\frac{R}{Q}} \cos \phi - (1 - e^{(t-t_1)/t_c})I_{\text{beam}}Q_L\frac{R}{Q}.$$

Equation 100 shows us that we have a problem: the excitation driven by the RF source changes its phase with respect to the beam, but the beam-driven excitation is always purely decelerating. In the case of $\phi = 0$, Equation 100 will result in the unloaded voltage and the loaded voltage exactly compensating each other for all times $t > t_1$; since the first voltage is now reduced but the second voltage is not reduced, the result is that for $t > t_1$, the net phase and voltage in the cavity vary. Meanwhile, the slope of the voltage is given by:

$$\frac{dV}{d\phi} = -2(1 - e^{-t/t_c})\sqrt{Q_L P\frac{R}{Q}} \sin \phi. \tag{101}$$

In other words, the voltage slope does not change with the buildup of beam loading, but the net decelerating voltage does change.

How is this situation to be handled? In other words, given that we want the voltage seen by the beam to be $V_0 \cos \phi$, and the slope of the voltage to be $-V_0 \sin \phi$, and that we want these values to hold for all time, what should we do? The prescription is as follows:

- From $t = 0$ to $t = t_1$, use the RF power source at its nominal power P_{in} and phase phi to achieve an initial cavity voltage V_0 at the desired phase;

- At $t = t_1$, turn off the RF source, and reactivate it with a new power P_1 and phase ϕ_1, such that the new power and phase will correctly compensate the loading voltage.

The first item of the prescription, at least, sounds simple! We can accomplish the second item by considering the voltage for $t > t_1$ as the superposition of 3 fields: the initially-established field, which is now decaying exponentially; the field from the beam; and the field from the RF power source. Putting this mathematically:

$$V(t > t_1) = e^{-(t-t_1)/t_c}V_0 \cos \phi + 2(1 - e^{-(t-t_1)/t_c})\sqrt{Q_L P_1\frac{R}{Q}} \cos \phi_1 \tag{102}$$

36

$$- (1 - e^{-(t-t_1)/t_c})I_{\text{beam}}Q_L\frac{R}{Q},$$

$$\frac{dV}{d\phi}(t > t_1) = -e^{-(t-t_1)/t_c}V_0 \sin\phi - 2(1 - e^{-(t-t_1)/t_c})\sqrt{Q_L P_1 \frac{R}{Q}}\sin\phi_1.$$

We know that we want $V = V_0 \cos\phi$ for all time, and we want $dV/d\phi = -V_0 \sin\phi$ for all time. Including that constraint, we find the following expressions:

$$\left[1 - e^{-(t-t_1)/t_c}\right]\left(2\sqrt{Q_L P_1 \frac{R}{Q}}\cos\phi_1 - I_{\text{beam}}Q_L\frac{R}{Q} - V_0\cos\phi\right) = 0, \tag{103}$$

$$\left[1 - e^{-(t-t_1)/t_c}\right]\left(\sqrt{Q_L P_1 \frac{R}{Q}}\sin\phi_1 - V_0\sin\phi\right) = 0.$$

Remarkably, we see that a single value of P_1 and a single value of ϕ_1 will suffice for all $t > t_1$! We merely have to solve the equations

$$2\sqrt{Q_L P_1 \frac{R}{Q}}\cos\phi_1 - I_{\text{beam}}Q_L\frac{R}{Q} - V_0\cos\phi = 0, \tag{104}$$

$$\sqrt{Q_L P_1 \frac{R}{Q}}\sin\phi_1 - V_0\sin\phi = 0$$

for P_1 and ϕ_1. This is the solution of two equations with two unknowns, which is straightforward if tedious due to numerous trigonometric functions and square roots.

7.2 Single-Bunch Beam Loading

Beam loading also occurs within a single bunch – loading from the head of the bunch decreases the accelerating voltage available to the particles in the tail of the bunch. Such loading is typically described as a *wakefield*, in other words an induced field that is left in the "wake" of the bunch. The single-bunch loading can also be modeled as the shock excitation of all of the accelerating modes of the cavity by the beam.

Calculation of the longitudinal wakefield is a difficult process in that the bunch is usually short compared to any other dimension in the problem (RF wavelength, cell length, cell diameter, aperture radius), and thus there are very serious speed-of-light and causality issues which enter into the estimate. A convenient formula for estimation of the wakefield is provided by Bane *et. al* [17]: the decelerating electric field a distance z behind a particle of charge q is given by $E_{\text{wf}} = qW_L(z)$, where

$$W_L(z) = \frac{Zc}{\pi a^2}\exp\left(-\sqrt{\frac{z}{s_z}}\right), \text{ where} \tag{105}$$

$$s_z \approx 0.41\frac{a^{1.8}g^{1.6}}{d^{2.4}},$$

and a is the aperture radius of the iris, g is the interior width of the cell, and d is the cell period (i.e., $g = d - h$, where h is the disc thickness); Z is the impedance of the medium, which is the canonical 377 Ω for an evacuated accelerator structure.

7.2.1 Self-Loading

In the previous discussion of single-bunch loading, a formula for the decelerating voltage behind a charge is provided. That formula has a nonzero value for $z = 0$, indicating that a single electron can experience a wakefield from its own passage!

To understand this, consider a thought experiment proposed by Wangler [18], in which two particles with charge q and energy U_0 in each pass through a resonant cavity with frequency ν, and there is a longitudinal distance $c/2\nu$ between the two particles. At the start of the experiment there is no stored energy and therefore no voltage in the cavity. The first particle passes through the cavity and induces a voltage $-V_b$ in its wake (decelerating, as indicated by the sign). The voltage can only be established if the cavity stores some amount of energy $R_{cav}V_b^2$, which by conservation of energy must be removed from the first particle; $U_1 = U_0 - R_{cav}V_b^2$. We can also equate the loss of energy in the first particle to a decelerating voltage, $U_1 = U_0 - qV_1$. Note that V_1 is not required to be equal to V_b.

Now the second particle passes through, but at a time difference such that the field in the cavity is now an accelerating field with voltage V_b. Since the second charge is identical to the first, it will leave in its wake a decelerating voltage $-V_b$ which cancels the voltage left by the first particle, so after the second particle is gone the cavity is once again empty of energy and at zero voltage. However, the second particle has also been accelerated by the voltage left by the first, hence $U_2 = U_0 - qV_1 + qV_b$.

Now: since the cavity is empty, and energy is conserved, we know that the total energy in the two particles must be $2U_0$. Therefore, $qV_b - 2qV_1 = 0$, or $V_1 = V_b/2$. That is to say, a point charge experiences half of the energy loss indicated by the $z = 0$ wakefield. This is the *fundamental theorem of beam loading*.

7.2.2 Single-Bunch Loading Compensation

In general the effect of the single-bunch loading can be computed by convolving the wakefield W_L with the RMS bunch shape, but some semi-quantitative understanding of the interaction is always welcome. We can achieve this understanding by modelling the bunch with 2 macroparticles: one with charge $q/2$ at $z = 0$, and another with charge $q/2$ at $z = 2\sigma_z$, thus giving the overall distribution an RMS length of σ_z. The decelerating voltage experienced by each particle is given by:

$$
\begin{aligned}
V_1 &= \frac{Lq}{4}W_L(0), & (106)\\
V_2 &= \frac{Lq}{4}W_L(0) + \frac{Lq}{2}W_L(2\sigma_z),\\
&= \frac{Lq}{4}W_L(0)(1 + 2e^{-\Delta}),
\end{aligned}
$$

where $\Delta = \sqrt{2\sigma_z/s_z}$ and L is the cavity length. The resulting average and RMS energy loss are given by:

$$
\begin{aligned}
<V> &= \frac{Lq}{4}W_L(0)(1 + e^{-\Delta}), & (107)\\
\sigma_V &= \frac{Lq}{4}W_L(0)e^{-2\Delta}.
\end{aligned}
$$

Thus, both the average and the RMS deceleration are worse for short bunches than for long, which makes intuitive sense. Also, for very short bunches, when $\Delta \to 0$, the mean energy loss goes to $LqW_L(0)/2$, as required by the fundamental theorem of beam loading.

The RMS energy spread term arises from the fact that the second macroparticle is decelerated by the voltage left in the wake of the first macroparticle, as well as by the self-loading term. We can compensate this effect by adjusting the relative phase of the accelerating field in such a way that the bunch is not riding on the crest of the wave, but slightly ahead of the crest. This will impart a greater voltage to the tail of the bunch than to the head, and through careful adjustment of the phase the effect of single-bunch loading and the effect of the acceleration can be made, in first order at least, to cancel.

What phase is required to compensate the beam loading? If the bunch centroid is accelerated at phase ϕ, then the first macroparticle is at phase $\phi - 2\pi\sigma_z/\lambda$, while the second is at phase $\phi + 2\pi\sigma_z/\lambda$. We can equate the change in energy gain by the two macroparticles to the change in deceleration due to wakefields:

$$V[\cos(\phi - 2\pi\sigma_z/\lambda) - \cos(\phi + 2\pi\sigma_z/\lambda)] = \frac{Lq}{2}W_L(0)e^{-\Delta}. \tag{108}$$

We can apply appropriate trigonometric identities and find:

$$\sin\phi = \frac{LqW_L(0)e^{-\Delta}}{4V}\frac{1}{\sin(2\pi\sigma_z/\lambda)}. \tag{109}$$

A reasonable approximation for $V \gg LqW_L(0)$, $\sigma_z \ll s_0$, and $\sigma_z \ll \lambda$ is:

$$\phi = \frac{LqW_L(0)}{8\pi V}\frac{\lambda}{\sigma_z}. \tag{110}$$

Since running far off-crest reduces the average energy gain even further, it is worthwhile to note that a high voltage, low charge, long bunch, or short RF wavelength all reduce the distance the bunch must be from the RF crest.

8 The ILC Accelerating Cavity

So far we have concentrated on the theory of accelerating cavities, with an emphasis on superconducting accelerators operating in the π mode. Now we can turn our attention to the real design of the accelerating cavity which is to be used in the International Linear Collider. Note that many of the parameters will be much more fully discussed in later lectures, in particular the lecture on superconducting RF.

8.1 Basic Cavity Parameters

In Section 5.1.1, we saw that the surface resistance of superconductors is proportional to the square of the operating frequency, which means that a lower frequency is strongly desired. On the other hand: in Section 3, we saw that the diameter of the cavity, and thus its cost, is linearly proportional to frequency; in Section 6.1, we saw that the filling time is inversely proportional to frequency. Since we want to build a cavity with a low surface resistance, small size, and short filling time, these requirements are in conflict with one another, so a compromise is required. The compromise frequency of operation is $\nu = 1.3$ GHz. At this frequency, and considering the requirement that the phase velocity be matched to the speed of light, the length of one cell (or length of one half wavelength) is 0.1154 meters. The number of cells per cavity is similarly a compromise: on the one hand, using a large number of cells per cavity reduces the number of couplers of all types, but increases the complexity of the electrical design of the cavity and its sensitivity to errors. The
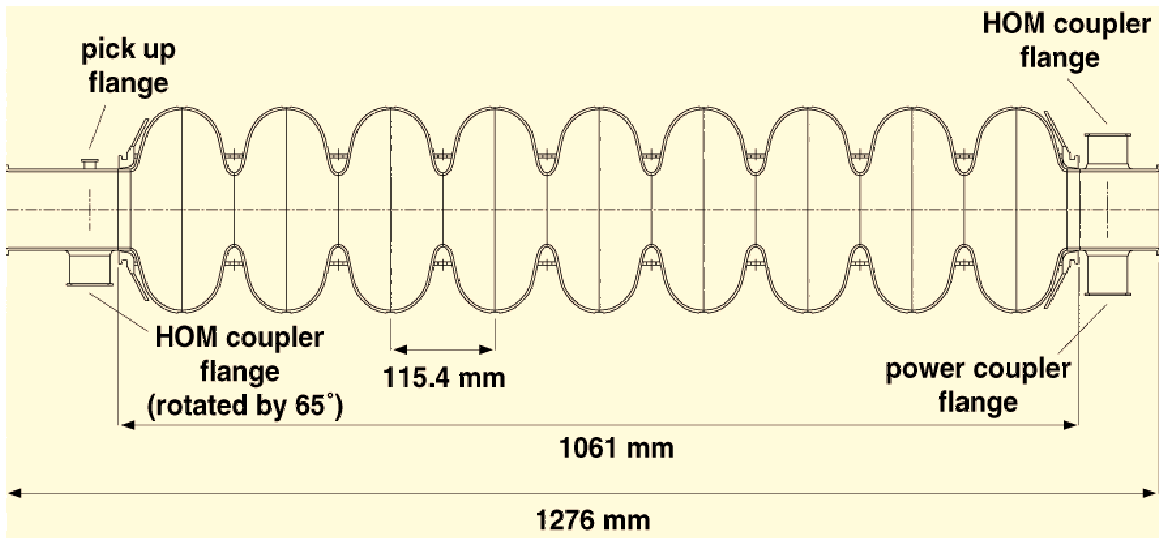
Figure 13: Cutaway diagram of the ILC baseline RF cavity.

compromise solution is 9 cells, for a total active length of about 1.04 meters. Figure 13 shows a cutaway diagram of the ILC baseline cavity.

The R/Q of the ILC cavity is 1036Ω. Figure 14 shows the surface resistance of an ILC cavity as a function of temperature. The surface resistance is dominated by the AC resistivity of super-conducting niobium down to about 1.8 K, at which point the residual resistivity of the material impurities and handling become dominant. From Figure 14 we see that there is little benefit to operating the ILC cavities significantly below 2 K, and so 2 K is their operating temperature.
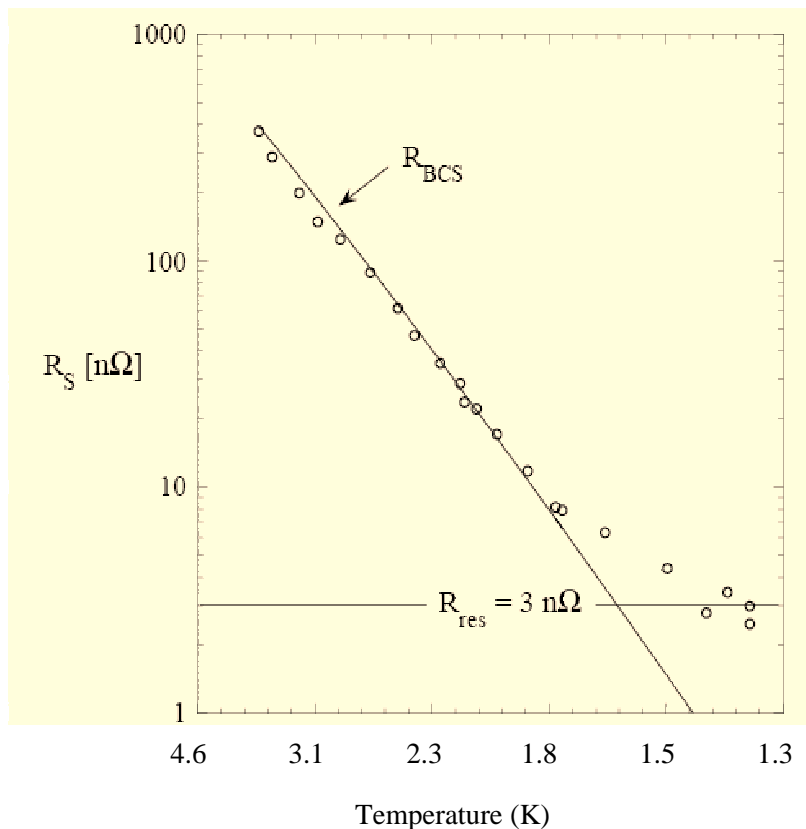

Figure 14: Surface resistance of an ILC cavity as a function of operating temperature.

Figure 15 shows the wall Q as a function of the accelerating gradient. At low gradients the wall Q approaches the expected value of about 2×10^{10} for a 1.3 GHz cavity at 2 K. At higher gradients, for a number of reasons, the wall Q decreases. At even higher gradients, around 43 MV/m, a cavity with the geometry of the ILC cavity develops fields comparable to the critical magnetic field and leaves the superconducting state ("quenches"). Thus, the gradient is not a completely free parameter. The operating gradient is selected based on the following tradeoffs:

- Raising the gradient reduces the length of the linac, thus reducing the number of cavities, length of tunnel, etc. Thus, increasing the gradient reduces the cost.

- Raising the gradient increases the power dissipation at 2 K, which increases the cost of the refrigeration system which is needed to remove the heat from the cryogenic system. Thus, raising the gradient increases the cost.

41

- The maximum gradient which a cavity can sustain is not the same for all cavities: some cavities can operate with very high gradients, while other cavities which have been constructed using the same processes will have lower limits. Thus, raising the gradient can increase the system cost, since it increases the number of cavities which are constructed and rejected.
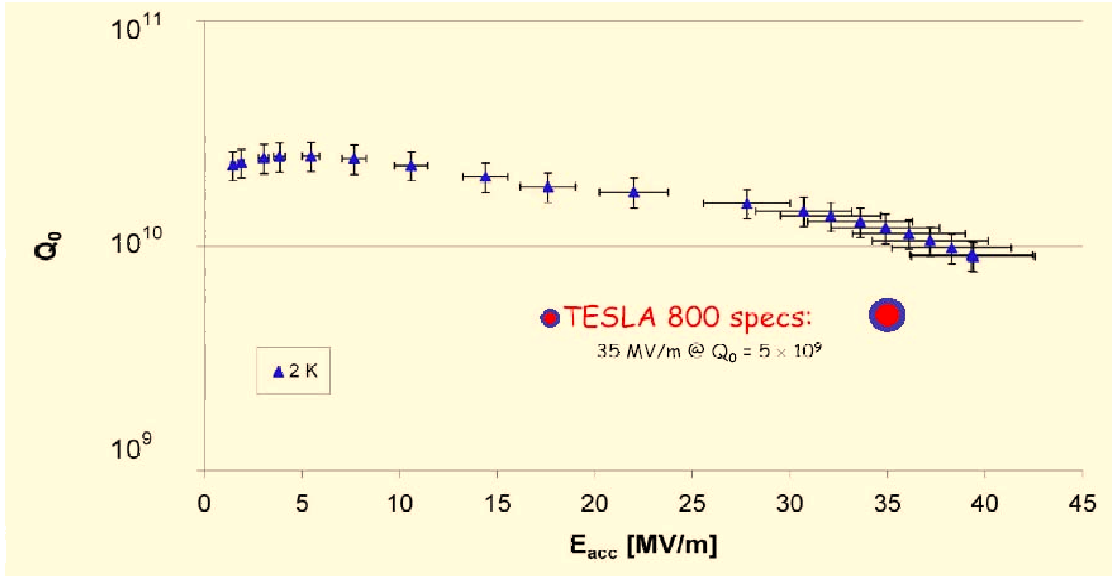

Figure 15: Wall Q of an ILC cavity as a function of gradient.

Considering just the cryogenic system costs and the capital costs, one finds that the ILC linac costs are minimized for a gradient of about 42 MV/m, with the exact minimum depending somewhat on the assumptions made about how the wall Q varies with gradient. The mean maximum operable gradient for ILC-style cavities constructed to this point is much lower, around 28 MV/m. The cost minimum is fortunately rather broad, and so a gradient of 31.5 MV/m has been selected. This gradient causes an increase in the ILC's cost of about 3%, while representing an incremental improvement over achieved gradients to date (as opposed to 42 MV/m, which is a 50% improvement over current performance).

With R/Q of 1036Ω and a wall Q of about 10^{10}, the shunt impedance of the ILC structure is close to $10^{13}\Omega$. From the definition of shunt impedance, this implies a wall-power dissipation of about 110 watts per cavity when the cavity is filled to 31.5 MV/m.

8.2 Beam Current, Loaded Q, Duty Factor

Given a final beam energy of 250 GeV, it is clear that the average current of the ILC has to be fairly low. For example, if one decided to use currents comparable to the stored currents in one

of the B-factories (1-2 amperes), the beam power would be 250-500 GW – over 10 times the total power consumption of the state of California! The selected average current of 45 μA yields power per beam of just over 11 MW, or 22 MW when both beams are considered. This is more reasonable, if still large.

What format should the beam have – train length, duty factor, etc.? One option would be to have a 100% duty factor – a continuous current of 45 μA. At this low current, the power transferred to the beam is about 1.5 kW, meaning that the power dissipated in the cavity walls (the aforementioned 110 W) is no longer negligible. Worse, it means that the average power dissipated in each linac is about 800 kW. Removing 800 kW of heat from a 2 K system would require around 600 MW of refrigeration power per linac. In order to achieve efficient operation, we want the refrigeration requirements of each linac to be small compared to the beam power. This is accomplished by reducing the duty factor, and therefore raising the beam current above the average current by some factor. This implies that a duty factor no larger than (11 MW)/(600 MW) = 0.0167 should be considered, or equivalently that no beam current below 2.7 mA should be considered.

At the other end of the spectrum, it is necessary to use a damping ring to achieve the low transverse emittances which are required if we are to achieve a luminosity of 2×10^{34}cm^{-2}sec^{-1} with an average current of just 45 μA. For bunched electron beams, storage ring currents of 1-2 amperes are the contemporary operating limit. Thus, we find that the acceptable range of beam currents for the ILC is bounded at the lower end by about 3 mA and at the upper end by about 2 A.

The ILC parameters call for a beam current of 9 mA. This is actually rather close to the low end of the range described above. This was chosen because, as we shall see, use of a low beam current and a high duty factor (1/200) makes the bunch train extremely long; this is advantageous for reasons which are obvious (making measurements and applying corrections to cavity properties, beam orbits, etc.), and for reasons which are not obvious (which we will discuss in the linac transverse dynamics lecture tomorrow).

With the voltage (32.8 MV) and the beam current (9 mA) chosen, it becomes possible to compute the necessary RF power input to each cavity (295 kW) and the loaded Q (3.52×10^6). Thus the e-folding time of the cavity t_c is 862 μsec, and the fill time before introducing the beam is 597 μsec. Since none of the energy used to fill the cavity is transferred to the beam, but all of the energy put out by the RF sources during beam time is absorbed by the beam, we want the bunch train length to be at least longer than the fill time for efficient operation, and ideally as long as possible. The train length selected for the ILC is just under 1 msec, which is not enormously longer than the fill time; unfortunately, lengthening the train while keeping the beam current at its constant 9 mA requires either longer trains in the damping ring (driving up the damping ring cost as their length increases), more bunches in the damping ring (driving up the damping ring currents and associated instabilities and costs), or higher-charge bunches in the damping ring (which would cause beam-beam instabilities at the IP, and cause other problems which will be discussed tomorrow). With 1 ms trains and a 1/200 duty factor, the ILC has a repetition rate of 5 Hz.

8.3   Single-Bunch Loading Compensation

The aperture radius of the ILC cavity is 35 mm, which implies a value of $W_L(0) \approx 2.9 \times 10^{13}$ V/C/m. The single bunch charge in the ILC is about 3.2 nC, and the RMS bunch length is 300 μm. From Equation 110, the bunch needs to be kept about 5.2° off-crest to compensate the single-bunch loading.

8.4 Bandwidth, Tuning, and Lorentz Force Effects

With a loaded Q of 3.5×10^6, the bandwidth of the ILC cavity is ν/Q_L, which is about 370 Hz. Matching the resonant frequency of a cavity to the level of 1 part per million is not achievable from first principles – Equation 64 implies that frequency shifts of this magnitude can be caused by micrometer scale errors in the cavity hole size a. For this reason, each ILC cavity has a mechanical tuner which can be used to deform the cavity slightly, thus shifting its resonant frequency. The tuner is used to achieve the initial adjustment of the frequency to 1.3 GHz, and also to correct for small errors that enter over time due to settling or other slow mechanical distortions.

The cavity tuner has an additional role: for cavities which are not powered, the tuner is used to change the resonant frequency of the cavity away from any frequency which is resonant with the beam. This is necessary because, as we have seen, otherwise the beam will induce a time-dependent voltage which will grow over the length of the bunch train until it is almost equal to the nominal cavity voltage!

An additional issue is the deformation of the cavity itself due to electromagnetic forces during operation. When the cavities are filled with energy, the fields generate radiation pressure which acts on the walls. The resulting deformation changes the frequency of the cavity. This is known as "Lorentz Force Detuning."

The first line of defense against Lorentz force detuning is to make the cavity mechanically stiffer, and the ILC cavities have stiffening rings around their irises for this purpose. The stiffening rings reduce the sensitivity of the cavities to a level of $1 \text{ Hz}/(\text{MV/m})^2$ [20]. At 31.5 MV/m, the resulting detuning is around 1 kHz, which is still several times the bandwidth of the system. The use of mechanical stiffness is ultimately limited by the fact that changes to the cavity which make it stiffer, such as stiffening rings, also tend to reduce the thermal conductivity between the inner walls of the cavity and the surrounding liquid helium bath.

The next line of defense, for the ILC cavities, is piezoelectric tuners. These are tuners which have a very small range compared to the main tuners, but which can operate within the millisecond RF pulse to maintain the desired resonant frequency of the cavity. Tests have shown that piezoelectric tuners can maintain the cavity resonant frequency within the 370 Hz bandwidth at gradients as high as 35 MV/m and even higher.

8.5 The ILC Standard RF Unit

Figure 16 shows a schematic of the standard RF unit for use in the ILC. Each RF unit includes: one RF power source; 26 9-cell cavities; a superconducting focusing quadrupole, superconducting steering dipoles, and a beam position monitor, constructed as a package; and a suitable cryogenic system for all of these devices.

In order to power 26 cavities at power levels of 295 kW, a total power of 7.7 MW is needed. The RF power source can produce a peak power fo 10 MW, which leaves some overhead for regulation, losses in the normal-conducting waveguides and distribution system, etc. Since the total length of the RF unit is large (about 38 meters), it is constructed in 3 "cryomodules," each of 12.7 meter length: there are 9 cavities in the first and third cryomodule in a unit, while the center cryomodule has only 8 cavities so as to leave room for the quadrupole package.

The beam energy at entry to the main linac is 15 GeV, and the desired final beam energy is 250 GeV. With each cavity contributing about 32.8 MeV, an RF unit of 26 cavities contributes about 850 MeV, and so a total of 276 RF units is needed in each linac. In actual fact, the positron linac has 278 RF units, and the electron linac has 282 RF units. The two additional units in the positron linac are needed because of short-range wakefield losses and operation 5° off-crest. The electron linac has these requirements as well, and also needs 4 RF units to make up the energy
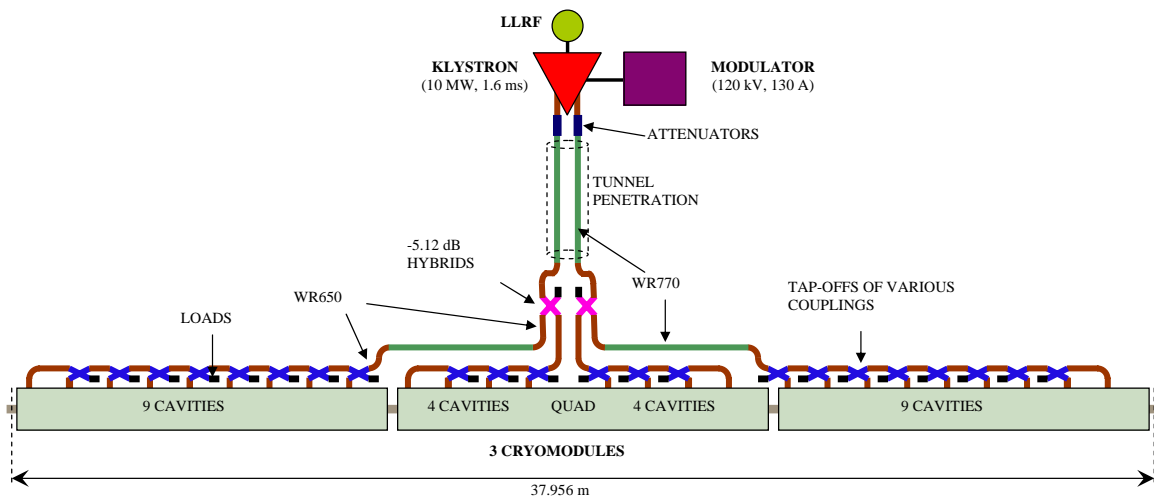
Figure 16: Schematic of an ILC RF unit.

losses generated by an undulator in the electron linac: this undulator generates photons which are used to make positrons.

A   Useful Constants and Numerical Values

Symbol	Description	Value	Notes
ϵ_0	Electric permeability of vacuum	8.85×10^{-12} F/m	
μ_0	Magnetic permittivity of vacuum	$4\pi \times 10^{-7}$ H/m	
c	Speed of light in vacuum	3.00×10^8 m/s	$\equiv 1/\sqrt{\epsilon_0 \mu_0}$
Z_0	Impedance of free space	377 Ω	$\equiv \sqrt{\mu_0/\epsilon_0}$
z_{01}	First zero of J_0 Bessel function	2.404	

B Longitudinal Field Components in an Infinite Conducting Pipe

This section goes through the grinding mathematics involved in solving for the longitudinal field components in an infinite conducting pipe of radius b, for which the setup and the result are shown in Section 2.2.

A solution for Equation 17 can be sought by separation of variables: define $E_{0,z}(r,\theta) \equiv R(r)\Theta(\theta)$, and expand the $\nabla_\perp^2$ operator (available in any decent textbook on PDE's or electrodynamics):

$$\frac{1}{r}\frac{\partial}{\partial r}\left(r\frac{\partial}{\partial r}R\Theta\right) + \frac{1}{r^2}\left(\frac{\partial^2}{\partial\theta^2}R\Theta\right) + k_c^2 R\Theta = 0. \tag{111}$$

The function R can be pulled out of the θ-derivative, and similarly the function Θ can be pulled out of the r-derivative:

$$\frac{\Theta}{r}\frac{\partial}{\partial r}\left(r\frac{\partial}{\partial r}R\right) + \frac{R}{r^2}\left(\frac{\partial^2}{\partial\theta^2}\Theta\right) + k_c^2 R\Theta = 0. \tag{112}$$

Dividing by $R\Theta$, multiplying by r^2, and rearranging terms yields:

$$\frac{r}{R}\frac{\partial}{\partial r}\left(r\frac{\partial R}{\partial r}\right) + k_c^2 r^2 + \frac{1}{\Theta}\left(\frac{\partial^2\Theta}{\partial\theta^2}\right) = 0. \tag{113}$$

Equation 113 shows that the terms with θ dependence and the terms with r dependence have been completely separated. We can advance the solution of Equation 113 by requiring that the two components be equal and opposite, defining separation constant $\mathcal{Q}$:

$$-\frac{1}{\Theta}\left(\frac{\partial^2\Theta}{\partial\theta^2}\right) = \frac{r}{R}\frac{\partial}{\partial r}\left(r\frac{\partial R}{\partial r}\right) + k_c^2 r^2 = \mathcal{Q}. \tag{114}$$

The two components of Equation 114 can be solved separately. The first component, which defines $\Theta(\theta)$, can be solved almost by inspection: $\Theta = \cos(n\theta + \theta_n)$, where $\mathcal{Q} = n^2$ and periodicity – the requirement that $\Theta(\theta) = \Theta(\theta + 2\pi)$ – constrains n to be an integer. This constraint can be inserted back into the other component of Equation 17:

$$= \frac{r}{R}\frac{\partial}{\partial r}\left(r\frac{\partial R}{\partial r}\right) + k_c^2 r^2 = n^2. \tag{115}$$

Multiplying through by R and expanding the derivative yields:

$$r^2 R'' + rR' + R(k_c^2 r^2 - n^2) = 0. \tag{116}$$

Equation 116 is *Bessel's equation of order n*; the solution is a linear combination of *Bessel Functions*

$$R = a_n J_n(k_c r) + d_n Y_n(k_c r). \tag{117}$$

Since $Y_n(0)$ diverges, we can limit ourselves to solutions for which $d_n \equiv 0$, and write down a solution for $E_{0,z}$ in terms of a series in n:

$$E_{0,z} = \sum_{n=0}^{\infty} a_n J_n(k_c r) \cos(n\theta + \theta_n). \tag{118}$$

C Solving for the Fields of a TM$_{np}$ Mode

Let us define our coordinate system such that $\theta_{np} \equiv 0$ for simplicity. We have four unknown components of the modal fields, and therefore 4 equations are required.

The θ component of the magnetic curl equation Tells us that $\partial H_{0,r}/\partial z - \partial H_{0,z}/\partial r = \epsilon \partial E_{0,\theta}/\partial t$. Since $H_{0,z} \equiv 0$ and we can replace time and longitudinal derivatives via Equation 13, we can write:

$$kH_{0,r} = -\epsilon \omega E_{0,\theta}. \tag{119}$$

The r component of the magnetic curl equation tells us that $1/r \partial H_{0,z}/\partial \theta - \partial H_{0,\theta}/\partial z = \epsilon \partial E_{0,r}/\partial t$. By similar operations to those in the previous paragraph, we find:

$$kH_{0,\theta} = \epsilon \omega E_{0,r}. \tag{120}$$

The θ component of the electric curl equation tells us that $\partial E_{0,r}/\partial z - \partial E_{0,z}/\partial r = -\mu \partial H_{0,\theta}/\partial t$. We can replace the time and longitudinal derivatives, and can also replace $E_{0,r}$ with $H_{0,\theta}$ via Equation 120 to find:

$$\frac{\partial E_{0,z}}{\partial r} = \frac{ik_c^2}{\omega \epsilon} H_{0,\theta}. \tag{121}$$

The magnetic divergence equation tells us that $\vec{\nabla} \cdot \vec{H}_0 = 0$. Since $H_{0,z}$ is identically zero, we can write:

$$\frac{\partial H_{0,\theta}}{\partial \theta} = -\frac{\partial}{\partial r} \left(r H_{0,r} \right). \tag{122}$$

Equation 121 can be used immediately to obtain $H_{0,\theta}$, which in turn allows $H_{0,r}$ to be determined from Equation 122 and $E_{0,r}$ from Equation 120. Finally, Equation 119 relates $E_{0,\theta}$ to $H_{0,r}$.

D Solution to the Horrendous Integral

Here is the detailed procedure for solving the messy integral in Equation 61,

$$\mathcal{I} = \int_0^a dr \frac{r^2 J_0(k_c r) J_0'(k_c r)}{\sqrt{a^2 - r^2}}. \tag{123}$$

The first step is to switch to a normalized variable, $\mathcal{R} \equiv r/a$, which recasts $\mathcal{I}$ as follows:

$$\mathcal{I} = -a^2 \int_0^1 d\mathcal{R} \frac{\mathcal{R}^2 J_0(k_c a \mathcal{R}) J_1(k_c a \mathcal{R})}{\sqrt{1 - \mathcal{R}^2}}, \tag{124}$$

where we have also replaced J_0' with $-J_1$. The new form does not appear to be much of an improvement, until one realizes that this permits a trigonometric substitution: $\int d\mathcal{R} f(\mathcal{R})/\sqrt{1 - \mathcal{R}^2} \equiv \int d\mathcal{X} f(\sin \mathcal{X})$, where $\sin \mathcal{X} = \mathcal{R}$. Replacing a bunch of Bessel functions with Bessel functions of trigonometric functions seems like a losing proposition, but one can then use the series expansion of the Bessel functions [21] to find:

$$\mathcal{I} = -a^2 \int_0^{\pi/2} d\mathcal{X} \sin^2 \mathcal{X} \left[1 - \frac{1}{4} k_c^2 a^2 \sin^2 \mathcal{X} + \frac{1}{64} k_c^4 a^4 \sin^4 \mathcal{X} - ... \right] \left[\frac{1}{2} k_c a \sin \mathcal{X} - \frac{1}{16} k_c^3 a^3 \sin^3 \mathcal{X} + ... \right]. \tag{125}$$

Since $k_c a$ is proportional to a/b, we can neglect any term with a power of $k_c a$ above that of the lowest order present. Neglecting all but the lowest order in $k_c a$ transforms our integral to:

$$\mathcal{I} \approx -a^2 \int_0^{\pi/2} d\mathcal{X} \frac{1}{2} k_c a \sin^3 \mathcal{X}, \tag{126}$$

and this form is convenient for "integration by table," yielding [23]:

$$\mathcal{I} \approx -\frac{1}{3} k_c a^3. \tag{127}$$

E Useful Bessel Function Identities

These identities can be found in D. Jackson's *Fourier Series and Orthogonal Polynomials* [5, 22].

$$\int_0^1 \mathcal{R}d\mathcal{R}[J_n(\mathcal{QR})]^2 = \frac{1}{2}\left\{[J_n'(\mathcal{Q})]^2 + \left(1 - \frac{n^2}{\mathcal{Q}^2}\right)[J_n(\mathcal{Q})]^2\right\} \tag{128}$$

$$J_n'(\mathcal{Q}) = \frac{1}{2}[J_{n-1}(\mathcal{Q}) - J_{n+1}(\mathcal{Q})]$$

$$J_{n+1}(\mathcal{Q}) + J_{n-1}(\mathcal{Q}) = \frac{2n}{\mathcal{Q}}J_n(\mathcal{Q})$$

$$J_0'(\mathcal{R}) = -J_1(\mathcal{R}).$$

References

[1] J. D. Jackson, *Classical Electrodynamics,* 2nd. Ed, p. 818 (1975).

[2] J. R. Reitz, F. J. Milford, R. W. Christy, *Foundations of Electromagnetic Theory,* pages 344-347 (1980).

[3] Jackson, *Classical Electrodynamics*, p. 236.

[4] J. R. Reitz, F. J. Milford, R. W. Christy, *Foundations of Electromagnetic Theory,* p. 365.

[5] D. Jackson, *Fourier Series and Orthogonal Polynomials*, pages 74 and 81 (1941).

[6] D. Whittum, private communication.

[7] T. Wangler, *RF Linear Accelerators,* page 59 (1998).

[8] E. L. Chu, *The Theory of Electron Linear Accelerators,* page 56 (1951).

[9] Jackson, *Classical Electrodynamics*, p. 126.

[10] Jackson, *Classical Electrodynamics*, p. 337.

[11] T. Wangler, *RF Linear Accelerators,* page 23 (1998).

[12] B. Aune *et al.*, *Physical Review Special Topics – Accelerators and Beams,* **3** 092001 (2000).

[13] G.A. Loew, R.B. Neal, "Electron Linacs: Theory," in P.M. Lapostolle, ed., *Linear Accelerators,* 65 (1970).

[14] T.I. Smith, "Standing Wave Modes in a Superconducting Linear Accelerator," HEPL-437 (1966).

[15] P. Wilson, "High-Energy Electron Linacs: Applications to Storage Ring RF Systems and Linear Colliders," SLAC-PUB-2884 (1982).

[16] C. Nantista, "Radio-Frequency Pulse Compression for Linear Accelerators," SLAC-Report-95-455 (1995).

[17] K.L.F. Bane, A. Mosnier, A. Novokhatski, K. Yokoya, "Calculation of the Short-Range Longitudinal Wakefields in the NLC Linac," in *ICAP 98 – Proceedings* (1998).

[18] T. Wangler, *RF Linear Accelerators,* page 297 (1998).

[19] T. Wangler, *RF Linear Accelerators,* page 295 (1998).

[20] P. Kneisel, private communication (2006).

[21] R. Haberman, *Elementary Applied Partial Differential Equations,* 2nd. Ed., page 234 (1987).

[22] D. Jackson, *Fourier Series and Orthogonal Polynomials*, pages 83 and 86 (1941).

[23] *Chemical Rubber Company Handbook of Chemistry and Physics,* 65th Ed., page A-59 (1984).